Guide for a field trip in the Modi Khola Valley (Central – Western Nepal): a complete transect of the Himalayan chain

GEOLOGICAL FIELD TRIPS AND MAPS

2025
Vol. 17 (1.3)

Guide for a field trip in the Modi Khola Valley (Central – Western Nepal): a complete transect of the Himalayan chain

https://doi.org/10.3301/GFT.2025.03

SOCIETÀ GEOLOGICA ITALIANA ETS
FONDATA NEL 1881 - ENTE MORALE R. D. 17 OTTOBRE 1885

ISPRA
Istituto Superiore per la Protezione e la Ricerca Ambientale

Sistema Nazionale per la Protezione dell'Ambiente

Geological Field Trips and Maps

Periodico semestrale del Servizio Geologico d'Italia - ISPRA e della Società Geologica Italiana ETS
Geol. F. Trips Maps, Vol.**17** No.1.3 (2025), 28 pp., 28 figs., 1 tab. (https://doi.org/10.3301/GFT.2025.03)

Guide for a field trip in the Modi Khola Valley (Central – Western Nepal): a complete transect of the Himalayan chain

Giorgia Carano[1]

[1] Politecnico di Torino, Department of Environment, Land and Infrastructure Engineering (DIATI), Corso Duca degli Abruzzi 24, 10129 Turin, Italy.

GC, 0009-0001-8092-585X.

Corresponding author e-mail address: giorgia.carano@polito.it

Cover page figure: dida

ISSN: 2038-4947 [online]

http://gftm.socgeol.it/

INDEX

INFORMATION

EXCURSION NOTES

ITINERARY

ABSTRACT

The Modi Khola valley in the Annapurna Region in central-western Nepal offers a unique opportunity to study the complete tectonic and metamorphic history of the area, thanks to the exceptional continuity and exposure of the outcrops and the excellent orientation with respect to the chain. The valley exposes an about 20 km transect of rocks belonging to the three main tectono-metamorphic units of the Himalayan chain. From the lower to the upper structural level it is possible to recognize: the medium-low grade metamorphic rocks of the Lesser Himalayan Sequence (LHS), the medium-high-grade metamorphic rocks of the Greater Himalayan Sequence (GHS), and the weakly or non-metamorphic rocks of the Tethyan Himalayan Sequence (THS). The main foliation in the three metamorphic units has a NW-SE trend and is generally dipping 40-45° towards N-NE. The metamorphic core of the chain, the GHS, is separated from the THS by the South Tibetan Detachment System (STDS; that in the area is named Mardi-Himal Detachment) with normal kinematics and from the LHS by the Main Central Thrust Zone (MCTZ) with reverse kinematics. In the Modi Khola area other intra-GHS discontinuities are present. From top to bottom: the Modi Khola Shear Zone (MKSZ), the Sinuwa Thrust (ST), the Bhanuwa Fault (BT).
The field trip itinerary covers 13 stops along the Modi Khola valley, providing insights into the tectonic and metamorphic evolution of the units. The excursion requires a medium-easy trek with a total altitude difference of 2630 m, spanning from Birethanti village (1500 m a.s.l.) to the Annapurna Base Camp (ABC; 4130 m a.s.l.). It is recommended to program at least 5 days to complete the itinerary. The guide emphasizes regional and local discontinuities, highlighting the importance of structural and microstructural analysis due to the complexity of the area and the limited evidence of deformation in the lithologies at outcrop-scale.
Overall, the Modi Khola valley is a remarkable place where the geological setting and the tectonic and metamorphic evolution of the Himalayan region can be investigated. This field guide provides valuable insights for both researchers and geology enthusiasts interested in understanding the complex geological evolution of central-western Nepal and to better appreciate the history of the highest mountain belt in the world.

Keywords: Modi Khola Valley, Himalayan chain, meso and microstructural analysis, field geology.

PROGRAM SUMMARY

The field trip is articulated in 13 stops (Tab. 1, Fig. 1) that is recommended to divide in minimum 5 days given the long distances and the slopes. Almost all stops are located along the path, so they are easily accessible. There are therefore no particular dangers in reaching them. However, the path is practically the only connecting route in the valley so it could be crowded with tourists and trekkers. The stops are organized in order to show a complete transect of the Himalayan chain crossing all its main tectono-metamorphic units, starting from the medium- to low-grade metamorphic rocks of the Lesser Himalayan Sequence, through the metamorphic core of the Greater Himalayan Sequence and ending in the structurally upper low-grade or non-metamorphic rocks of the Tethyan Himalayan Sequence.

SAFETY

Outcrops can be easily reached walking with no danger or particular access difficulties. However, the environment is a high mountain environment so proper clothing and proper equipment are strongly recommended. Hiking is not possible all year round due to the monsoon season which greatly affects the weather during the months between May and mid-October. Winter is also not recommended for cold

Tab. 1 - Summary of number, name and unit, latitude, longitude and altitude of the stops of the field trip.

Stop	Name and unit	Latitude	Longitude	Elevation (m)
1	Impure quarzites (LHS)	28°19'09.0''N	83°47'03.7''E	1088
2	Chlorite and sericite phyllites with blocks of quartzites (LHS)	28°20'19.6''N	83°47'58.5''E	1223
3	Ulleri Orthogneiss (LHS)	28°22'19.9''N	83°48'36.6''E	1859
4	Quartzites (LHS)	28°24'50.2''N	83°48'44.7''E	2150
5	Gneiss of Unit Ia (Lower GHS)	28°25'38.6''N	83°49'14.0''E	1924
6	Decimetric fold in the gneiss of Unit Ib (Upper GHS)	28°26'16.8''N	83°50'27.0''E	2451
7	Calcsilicatic gneiss of Unit II (Upper GHS)	28°28'22.4''N	83°52'23.1''E	2637
8	Migmatitic orthogneiss of Unit III (Upper GHS)	28°29'11.7''N	83°53'22.3''E	2883
9	Calcsilicatic gneiss of Unit IV (Upper GHS)	28°29'49.6''N	83°53'49.6''E	3033
10	Modi Khola Shear Zone evidence in the Unit IV (Upper GHS)	28°30'06.1''N	83°54'03.5''E	3158
11	Annapurna Yellow Formation (THS)	28°30'43.1''N	83°54'15.4''E	3414
12	Sanctuary Formation (THS)	28°31'18.1''N	83°54'27.4''E	3683
13	Machapuchare Fold (THS)	28°31'51.2''N	83°52'28.3''E	4130

temperatures at higher altitudes. It is therefore better to opt for autumn or spring season.

HOPITALS

Sewa Hospital and Research Centre, Pokhara 33700, Nepal, +97761528161

ACCOMODATION

For the overnight stay, along the entire length of the route there are several lodges. For the organization of this guide it is suggested to sleep in the following villages: day 1 Ghandruk, day 2 Chomrong, day 3 Dobhan, day 4 Machapuchare BC, day 5 Annapurna BC.

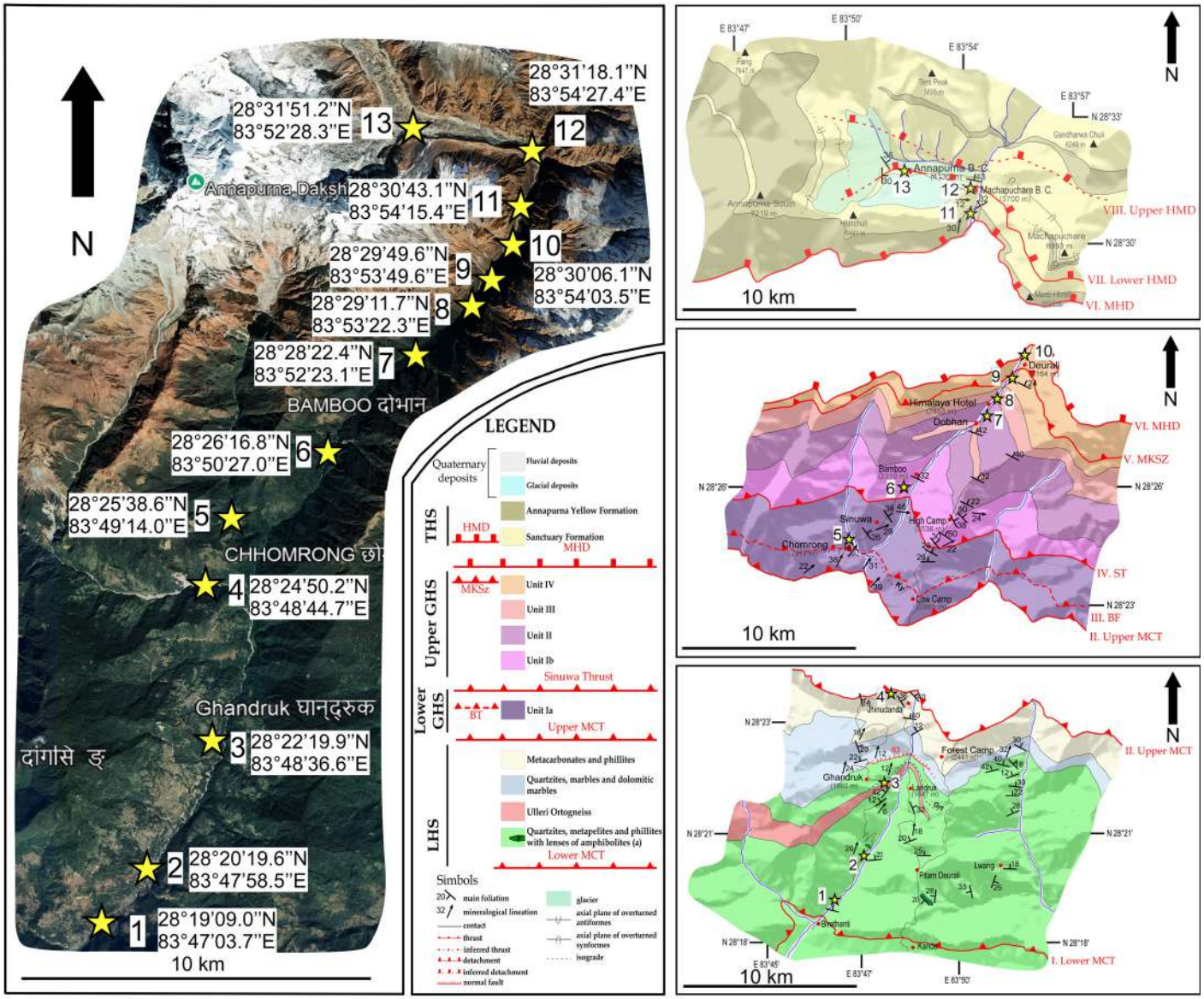

Fig. 1 - On the left, position of the stops (yellow stars) and relative coordinates in the Modi Khola valley on a satellite image from Google Earth; on the right position of the same stops on the geological map (1:200000) divided in the three main tectono-metamorphic units of the Himalayan chain, accompanied by legend. LHS: Lesser Himalayan Sequence; GHS: Greater Himalayan Sequence; THS: Tethyan Himalayan Sequence; MCT: Main Central Thrust; BF: Bhanuwa Thrust; ST: Sinuwa Thrust; MKSZ: Modi Khola Shear Zone; MHD: Mardi-Himal Detachment.

https://doi.org/10.3301/GFT.2025.03

INTRODUCTION

The Himalayan chain is the collisional orogeny *par excellence*, originating from the continental collision between the Indian plate and the Eurasian plate. Many of its peaks are the highest in the world. Although the chain has been studied for about two hundred years, since more or less the foundations have been laid for the theory of "Plate tectonics", its map coverage is still discontinuous and incomplete and this is certainly due to obstacles such as high altitudes, the steep slopes, the dense vegetation at lower altitudes, the scarcity of communication routes but also political problems. The obstacles, however, have not prevented the research and study of these territories that constitute a natural training ground for geologists and beyond.

The Modi Khola Valley, located in the Annapurna region, in Western-Central Nepal is the object of this field guide (Fig. 2). Along this ~20 km transect oriented N-S and orthogonal to the trend of the chain the main units of the Himalayan belt crop out. The metamorphic core of the Himalayan chain, the Greater Himalayan Sequence (GHS) is located between the low-grade or non-metamorphic rocks of the Tethyan Himalayan Sequence (THS) to the north and the medium- to low-grade metamorphic rocks of the Lesser Himalayan Sequence (LHS) to the south. Two of the main tectonic discontinuities of the Himalaya separate these units: the structurally lower Main Central Thrust Zone (MCTZ) with reverse kinematics and the structurally upper South Tibetan Detachment System (STDS) with normal kinematics. The MCTZ comprises the Lower MCT and the Upper MCT. In the Modi Khola area other intra-GHS discontinuities are documented (Hodges et al., 1996; Corrie and Kohn, 2011; Shrestha et al., 2020). From the top to the structurally bottom they are: the Modi Khola Shear Zone (MKSZ; 22.5-18.5 Ma; U-Pb dating on monazite, zircon and xenotime), the Sinuwa Thrust (ST; 27-23 Ma; U-Th-Pb dating on monazite and Lu-Hf on garnet), the Bhanuwa Fault (BT; 23-19 Ma; U-Th-Pb dating on monazite, Lu-Hf on garnet). Currently, the BT and the ST were identified only on the basis of petrochronological

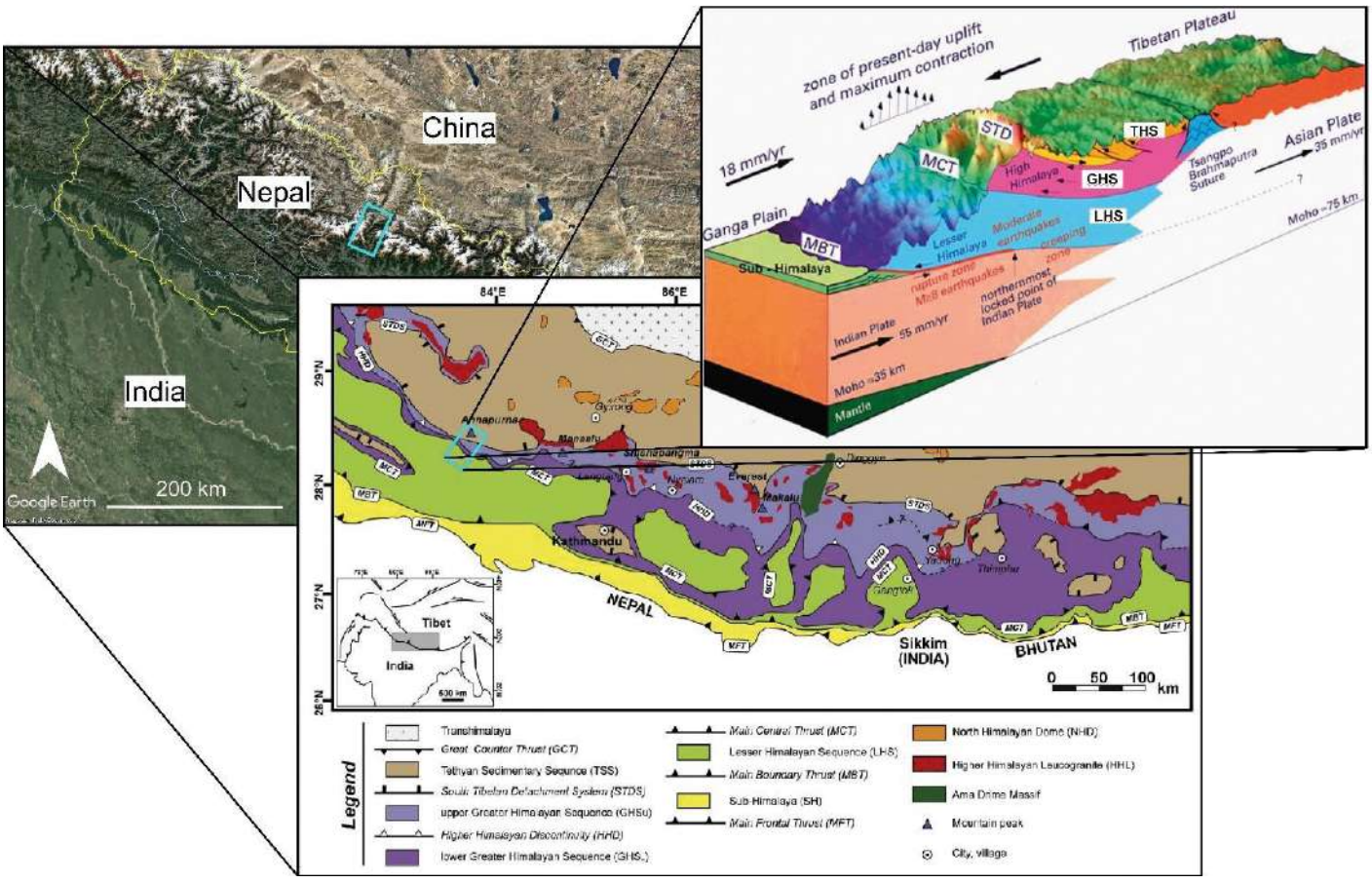

Fig. 2 - Location of the area of the field trip shown on satellite image (light blue rectangle; Google Earth); simplified geological map of the Himalayan chain and location of the area of this guide (light blue rectangle; modified from Carosi et al., 2018); structural diagram showing the main tectonic units and the main structures of the chain. THS: Tethyan Himalayan Sequence; GHS: Greater Himalayan Sequence; LHS: Lesser Himalayan Sequence; MBT: Main Boundary Thrust; MCT: Main Central Thrust; STD: South Tibetan Detachment (modified from Searle, 2013).

arguments, and their kinematics are debated. This guide is a journey that describes some of the main outcrops of the Modi Khola valley through the different units that make up the chain. The detailed description of the rocks starts from field observations and is further enriched through various micro and structural investigations, as these methods represent the best approach to gather information about the characteristics of these rocks. Due to their beauty and significance, many of these outcrops have been sampled by various research groups. Wherever possible, this guide also includes descriptions of these data, highlighting their importance. The new and recent observations at the mesoscale as well as the observations at the microscale allowed to draw up a detailed structural-geological map of the area and provided new and significant information regarding the kinematics of the tectonic discontinuities previously described in the literature and identified only on the basis of petrochronological evidence.

https://doi.org/10.3301/GFT.2025.03

GEOLOGY OF THE HIMALAYAN CHAIN

The Himalayan chain is considered the archetype of collisional orogeny (Le Fort, 1975) and is the youngest, longest and highest chain on Earth. It extends for a length of about 2500 km (Hodges, 2000) and has an arc geometry with an orientation about E-W, reaching widths up to 100-150 km.

The Himalayan chain is the result of the convergence and subsequent collision between the Indian and the Eurasian plates at ~59 Ma (Hu et al., 2016), after the closure of the Neo-Tethys sea, interposed between the two (Searle et al., 1987; Fig. 3). Following the continental collision, the deformation continued northward, resulting in a process of tectonic indentation (Tapponnier et al., 1982), which caused the lateral extrusion of southern China and Indochina (Fig. 4). The chain is characterized by a subduction slightly inclined dipping to N-NE in which the plate that subducts moves slightly faster than the upper plate; this results in a faster subduction compared to the shortening (Doglioni et al., 2007; Doglioni and Panza, 2015; Carosi et al., 2018).

The convergence rate between the Indian and Eurasian plates during the Neogene has been complex and variable over time. Earlier estimates suggested an average convergence of ~20 mm/yr for most of the Neogene, with a possible decrease to ~13–20 mm/yr from the Pliocene to the present (Powers et al., 1998; Lavé and Avouac, 2000). However, more recent models indicate higher total convergence rates: between ~44–57 mm/yr from 20 to 10 Ma and decreasing to ~34–44 mm/yr since 10 Ma (Molnar and Stock, 2009), while other studies propose a slowdown occurring prior to ~35 Ma, with convergence rates of ~40–50 mm/yr persisting since then (Copley et al., 2010). It is important to note that these values refer to total plate convergence. Modern geodetic data show that only part of this convergence is accommodated by crustal shortening across the Himalaya, with current rates in the central part of the chain—e.g., in central Nepal—estimated at ~17 mm/yr (Bilham et al., 1997; Larson et al., 1999), and more recently refined to ~17–21 mm/yr (Ader et al., 2012). The collision process is still in progress, as evidenced by the persistent seismicity of the area. The suture between the Indian and Eurasian plates is currently located in Tibet and is demarcated by the Indus-Tsangpo Suture Zone (ITSZ), which extends approximately 2000 km parallel to the Indus and Brahmaputra (Tsangpo in Tibetan) rivers with an E-W direction (Yin and Harrison, 2000).

The Himalayan chain *sensu strictu* is located south of the ITSZ and consists of sedimentary sequences between the Paleoproterozoic and the Eocene (Upreti et al., 2005), originally laid on the northern edge of the Indian plate. At regional scale, the architecture of the chain is fairly uniform and characterized by a high lateral continuity of the main tectonic structures, which have a general trend E-W. Local disturbances of the cylindrical structure of the chain occur in correspondence to the main tectonic windows: the windows of the Arun, Tamur and Tista in eastern Nepal and the window of Sikkim in north-eastern India (Goscombe et al., 2006) and the klippen (e.g., Kathmandu aquifer in central Nepal) (Upreti and Le Fort, 1999; Johnson et al., 2001).

It is widely accepted to divide the Himalayan chain into four main tectono-metamorphic units (Fig. 2). From the structurally bottom to the top are recognized:

– Sub-Himalaya Zone: comprising conglomerates, siltstones and sandstones deposited in the foreland basin.

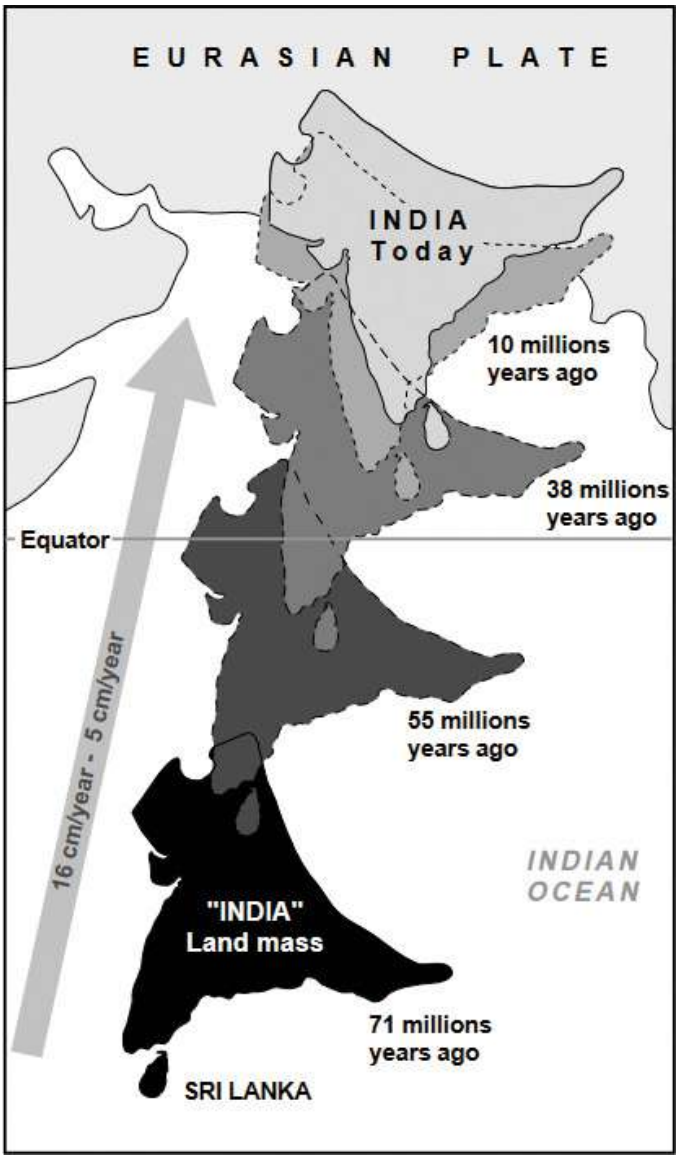

Fig. 3 - Northward drift and simultaneous anticlockwise rotation of the Indian plate from 71 Ma to present (modified from Dèzes, 1999).

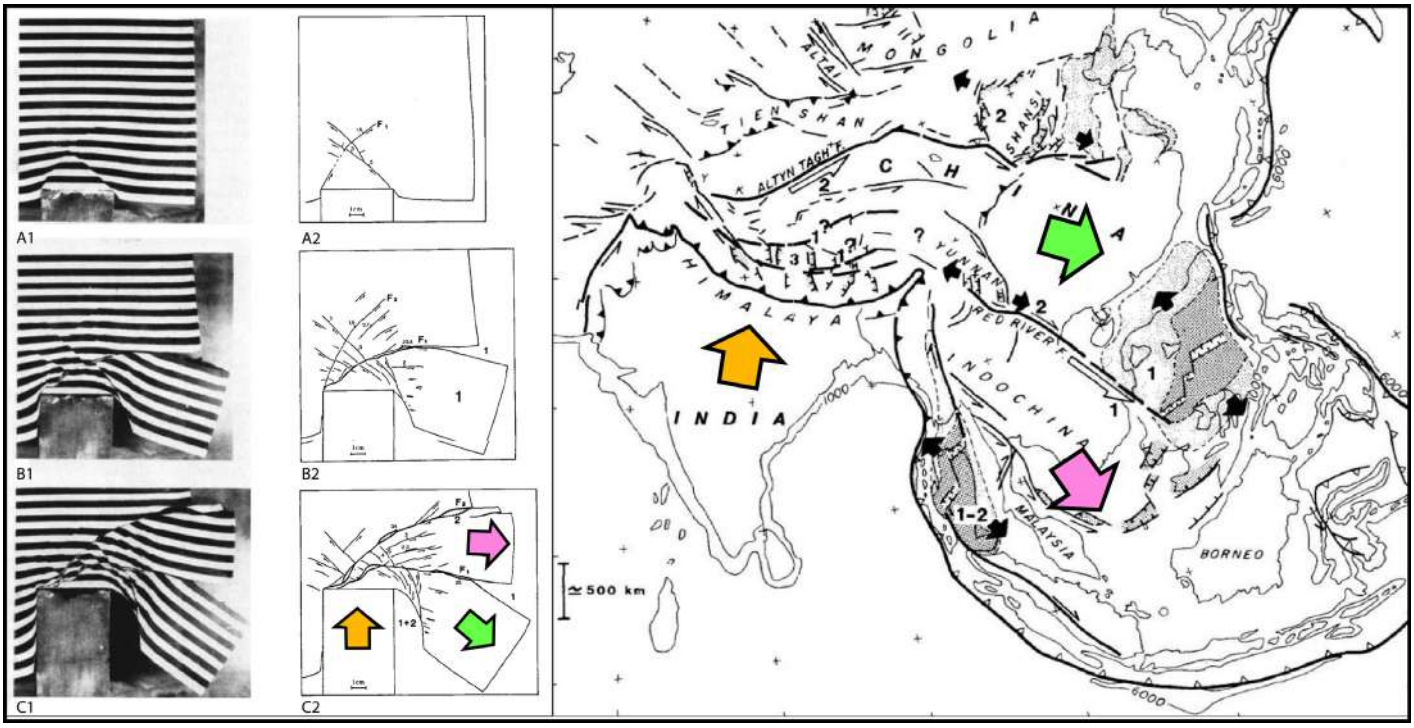

Fig. 4 - Left, experiment with plasticine specimen showing three successive indentation steps with only one lateral confinement. This results in the lateral extrusion of two blocks. Right, schematic map of Asia; the extruded blocks correspond to the territories of Indochina and southern China (modified from Tapponnier et al., 1982).

- LHS: characterized by very low metamorphic grade rocks to low temperature amphibolic facies rocks (Upreti, 1999; Hodges, 2000; Carosi et al., 2018) that are predominantly impure quartzites, marbles, phyllites, augen gneiss and metamorphosed mafic rocks (Gansser, 1964; Colchen et al., 1986; Hodges, 2000; Carosi et al., 2018) originally laid on the Indian passive margin (Gansser, 1964).
- GHS: metamorphic core of the chain mainly characterized by medium- high-grade metamorphic rocks derived from sedimentary and igneous protoliths (Hodges, 2000; Carosi et al., 2018).
- THS: Neo-Proterozoic (?)-Cambrian-Eocene marine sediments subsequently deformed under low- to very low-grade metamorphic conditions (Crouzet et al., 2007; Myrow et al., 2009; Antolín et al., 2011; Dunkl et al., 2011).

The aforementioned units are separated by tectonic discontinuities with regional significance that from the bottom to the top are (Fig. 2): the Main Frontal Thrust System (MFTS), the Main Boundary Thrust System (MBTS), the MCTZ and the STDS.

In the late 1990s, the recognition of normal faults (STDS) and reverse faults (MCTZ) within the same vertical section, respectively above and below the GHS, led to the formulation of new exhumation models for deep rocks (Hodges et al., 1992; Montomoli et al., 2013) based on synchronous activity along these contacts (Fig. 5).

The proposed models include channel flow (i.e., Beaumont et al., 2001; Godin et al., 2006), wedge extrusion (i.e., Grujic et al., 1996; Vannay and Grasemann, 2001), wedge insertion (i.e., Webb et al., 2007), and critical taper (Kohn, 2008). In all the models, it is noteworthy that the exhumation of the GHS is influenced by the activity along the tectonic contacts at its boundaries, the STDS at the roof and the MCTZ at the base.

Focusing only on these two main structures led to the interpretation of other internal tectonic structures (ductile shear zones) within the GHS, such as the Kalopani Shear Zone and the Modi Khola Shear Zone in Central Nepal or the Kakhtang thrust and the Laya thrust in Bhutan, as out-of-sequence thrusts (Montomoli et al., 2013), which were active subsequent to the combined action of MCTZ and STDS. Recently, additional structures have been identified within the GHS that were active prior to the MCTZ, including the High Himalayan Thrust in eastern Nepal, the Tojiem Shear Zone and the Mangri Shear Zone in western Nepal, and other discontinuities located between the Lower GHS and the Upper GHS (Montomoli et al., 2013, 2015). All these structures found within the GHS, along the entire length of the mountain range, suggest the existence of an important discontinuity known as the High Himalayan Discontinuity (HHD; Montomoli et al., 2013, 2015; Carosi et al., 2018). This has also led to a re-evaluation of previously proposed exhumation models. Furthermore, it has been emphasized that the Lower

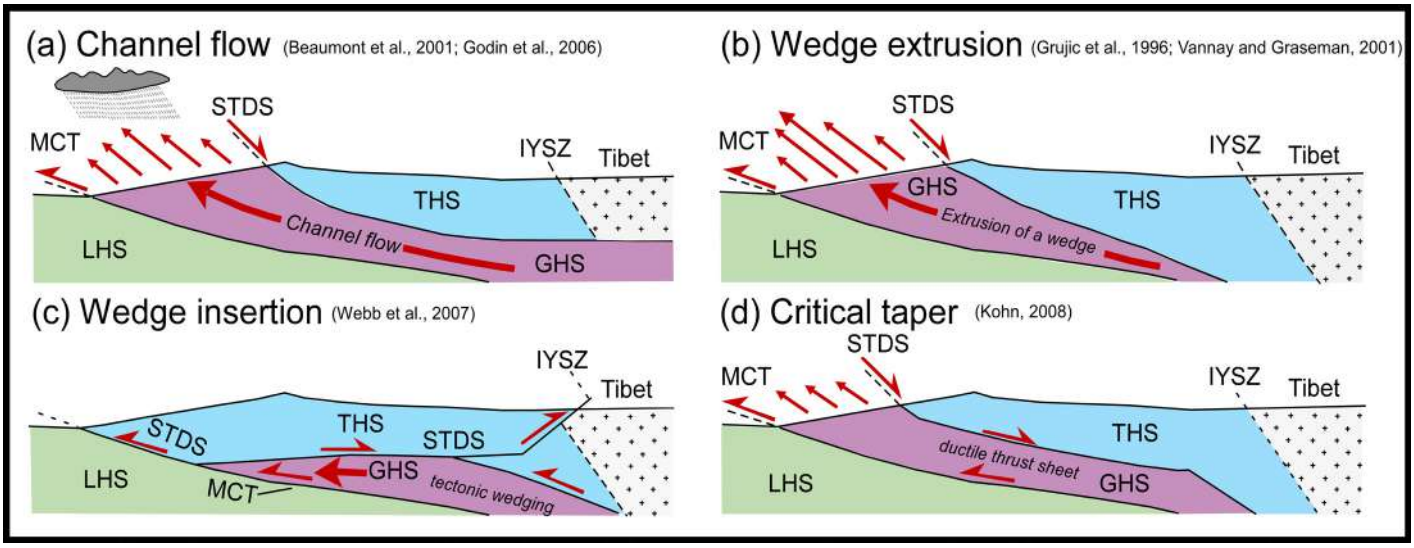

Fig. 5 - Schematic figure showing the main tectonic models currently proposed for the exhumation of the GHS. a. Channel flow model (Beaumont et al., 2001; Godin et al., 2006); b. Wedge extrusion model (Grujic et al., 1996; Vannay and Grasemann, 2001); c. Wedge insertion model (Webb et al., 2007); d. Model of the critical taper (Kohn, 2008). IYSZ: Indus-Yarlung Suture Zone; STDS: South Tibetan Detachment System; MCT: Main Central Thrust; THS: Tethyan Himalayan Sequence; GHS: Greater Himalayan Sequence; LHS: Lesser Himalayan Sequence (modified from Montomoli et al., 2013).

GHS and the Upper GHS reached their peak conditions at different stages and were likely exhumed with an estimated time lag of around 5 million years (Montomoli et al., 2013). As a result, a new exhumation model, the in-sequence shearing model, has been proposed (Fig. 6; Montomoli et al., 2015; Carosi et al., 2018). This model is based on the progressive activation of shear zones at progressively lower structural levels, leading to a rejuvenation of deformation towards the foreland. In view of these considerations, the stops in this field guide are essential for recognizing these internal discontinuities within the GHS.

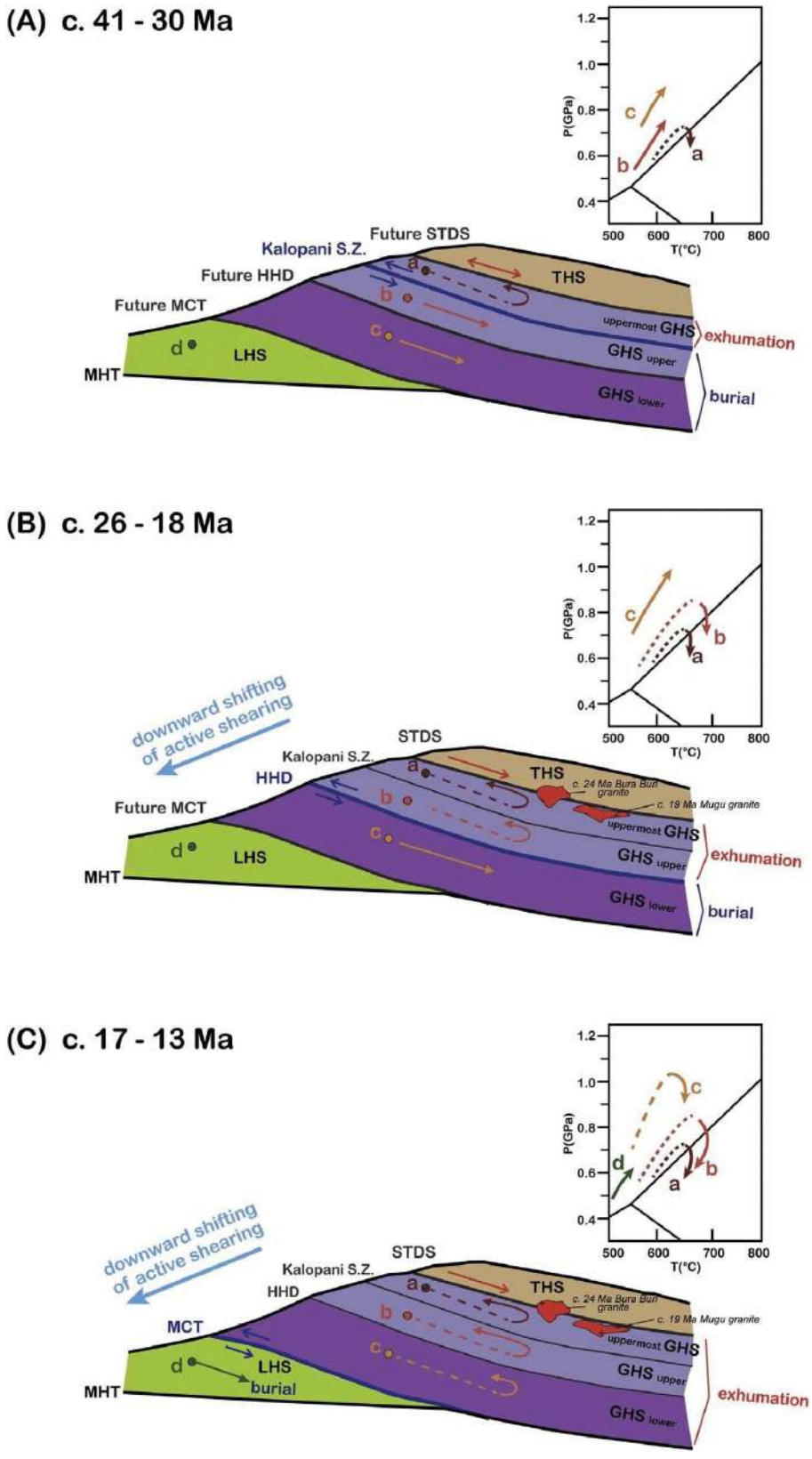

Fig. 6 - Schematic figure of the evolution of the chain according to the exhumative model of in-sequence shearing. A. 41-30 Ma, the MCT and the HHD are not yet active and the upper portion of the Upper GHS is exhumed by the action of the Kalopani Shear Zone, equivalent to the MKSZ as the structurally highest shear zone; note how the P-T path of the rocks located respectively in the hanging-wall and in the footwall of the structure is different. B. 26-18 Ma, the HHD, equivalent to the ST and separating the Upper and Lower GHS, is active and the remaining Upper GHS is exhumed; in this case the P-T path in the hanging-wall and in the footwall are different. C. 17-13 Ma, the MCT is active and the Lower GHS is exhumed. THS: Tethyan Himalayan Sequence; GHS: Greater Himalayan Sequence; LHS: Lesser Himalayan Sequence; HHD: High Himalayan Discontinuity; MCT: Main Central Thrust; MBT: Main Boundary Thrust; MHT: Main Himalayan Thrust (modified from Carosi et al., 2018).

GEOLOGICAL SETTING OF THE MODI KHOLA VALLEY

The Modi Khola valley has long been studied by researchers and this is certainly due to the good accessibility of the area and the fact that in this ~20 km transect, from S to N, and from bottom to the structurally top, rocks of the LHS, GHS and THS crop out (Hodges et al., 1996; Martin et al., 2005, 2010, 2015; Searle, 2010; Corrie and Kohn, 2011; Parsons et al., 2016a,b,c; Shrestha et al., 2020).

The lithologies in the valley present compositional layering and metamorphic foliation that are generally parallel, with a prevailing WNW-ESE direction and moderate dip towards N; this also applies to the tectonic discontinuities (Hodges et al., 1996).

In its southernmost part, the Modi Khola valley consists of the low-grade rocks of the LHS (chlorite metamorphic grade), in this area affected by the deformation of the MCTZ. The main lithologies are quartzites, metapelites and phyllites with amphibolite lenses and, shortly before the village of Ghandruk (1993 m a.s.l.), mylonitic augen gneiss (Ulleri Auctt.). In those rocks the main foliation is predominantly defined by muscovite and biotite. Moving structurally upwards, the high-grade rocks of the GHS crop out. These are commonly divided into three different units (Unit I, II, III; Hodges et al., 1996; Martin et al., 2010; Corrie and Kohn, 2011; Shrestha et al., 2020). However, based on our observations, we identify and map a fourth unit (Unit IV) in the upper part of the GHS, which differs from previous classifications and is discussed below. The rocks of Unit I are further subdivided into Ia, Ib and sometimes Ic (Corrie and Kohn, 2011). Unit Ia consists of muscovite-rich schist and gneiss alternating with quartzites, and is locally migmatitic. Unit Ib is composed of migmatitic schists and kyanite-bearing gneiss. In both Ia and Ib, the main foliation is defined by the iso-orientation of biotite and muscovite. Unit Ic, when present, comprises migmatitic rocks with segregated leucosomes, and garnet typically shows zoning with chemically homogeneous cores and manganese-enriched rims (Corrie and Kohn, 2011). However, lithologies corresponding to Unit Ic have not been identified in the studied transect. Unit II is characterized by marbles, calcsilicatic gneiss and biotite- and hornblende-bearing gneiss. Unit III consists of orthogneiss and gneiss with biotite and garnet locally migmatitic. Above the rocks of Unit III, calcsilicatic gneiss and marbles are present. These rocks, which are compositionally similar to Unit II, have been mapped differently from previous authors (Martin et al., 2005, 2010, 2015; Corrie and Kohn, 2011; Shrestha et al., 2020). Instead of being classified as Unit II, they have been assigned to Unit IV due to the presence of abundant leucogranitic intrusions, which are not frequent in Unit II.

Structurally above the GHS are the lower grade rocks of the THS. In the Modi Khola valley, these correspond to the rocks of the "Sanctuary Formation" made of metagreywackes and dark metapelites with intercalations of altered quartzites and yellowish limestones and rocks of the "Annapurna Yellow Formation", that are graded, well stratified marbles with intercalations of calcsilicatic levels and minor metarenites (Hodges et al., 1996). This last lithology, in the field, has a peculiar yellow-grey colour.

With respect to the discontinuities along the Modi Khola valley, the rocks affected by the deformation within the MCTZ are mainly attributed to the LHS, with a minor (~ 500 m) contribution from the Lower GHS (Martin et al., 2005, 2010, 2015).

In the case of the STDS, the oldest element described is represented by the Deorali Detachment characterized by a wide mylonitic zone (~300 m) and active from about 22.5 Ma (U-Th-Pb dating on zircon and monazite and $^{39}Ar/^{40}Ar$ on hornblende in the footwall of the Detachment; Hodges et al., 1996).

In the Modi Khola valley, the fabric related to the normal movement along the Deorali Detachment is obliterated by a reverse structure, SW vergent: the Modi Khola Shear Zone (MKSZ) with activity between 22.5-18.5 Ma (U-Th-Pb dating on zircon and monazite; Hodges et al., 1996), interpreted by Hodges et al. (1996) as an out-of-sequence thrust. After 18.5 Ma until ~14 Ma (Hodges et al., 1996), there is local extension along the Machapuchare Detachment (Mardi-Himal Detachment in this field guide).

In the valley, in addition to these main tectonic contacts, other intra GHS discontinuities are described in the literature; all of them with about parallel, WNW direction and dipping towards the N.

More specifically, Martin et al. (2010, 2015) provided P-T values for the transect that allowed to identify a new tectonic contact, the Bhanuwa Fault (BT), structurally higher than the MCTZ with normal kinematics. Subsequently, Corrie and Kohn (2011) reinterpret the Bhanuwa as a thrust (active from 23 to 19 Ma) and identify a further contact, the Sinuwa, also with reverse kinematics (active between 27 and 22 Ma). It is worth to mention that in the Modi Khola valley, the internal discontinuities of GHS are mostly cryptic, i.e. recognized on the basis of differences of paths P-T-t of adjacent rocky volumes.

https://doi.org/10.3301/GFT.2025.03

ITINERARY

The field trip consists of 13 stops (Figs. 1, 7 and Tab. 1) located in the Modi Khola valley in the Annapurna region in central-western Nepal. More specifically, the stops are between the village of Birethanti (1500 m a.s.l.) and the Annapurna Base Camp (ABC; 4130 m a.s.l.). The stops can only be reached through a trek of medium-easy difficulty making a total difference in altitude of 2630 m. For this reason, the excursion is divided into several days, minimum 5 days are recommended.

The guide aims to be of accompaniment through all the tectono-metamorphic units constituting the chain paying particular attention to regional and local discontinuities.

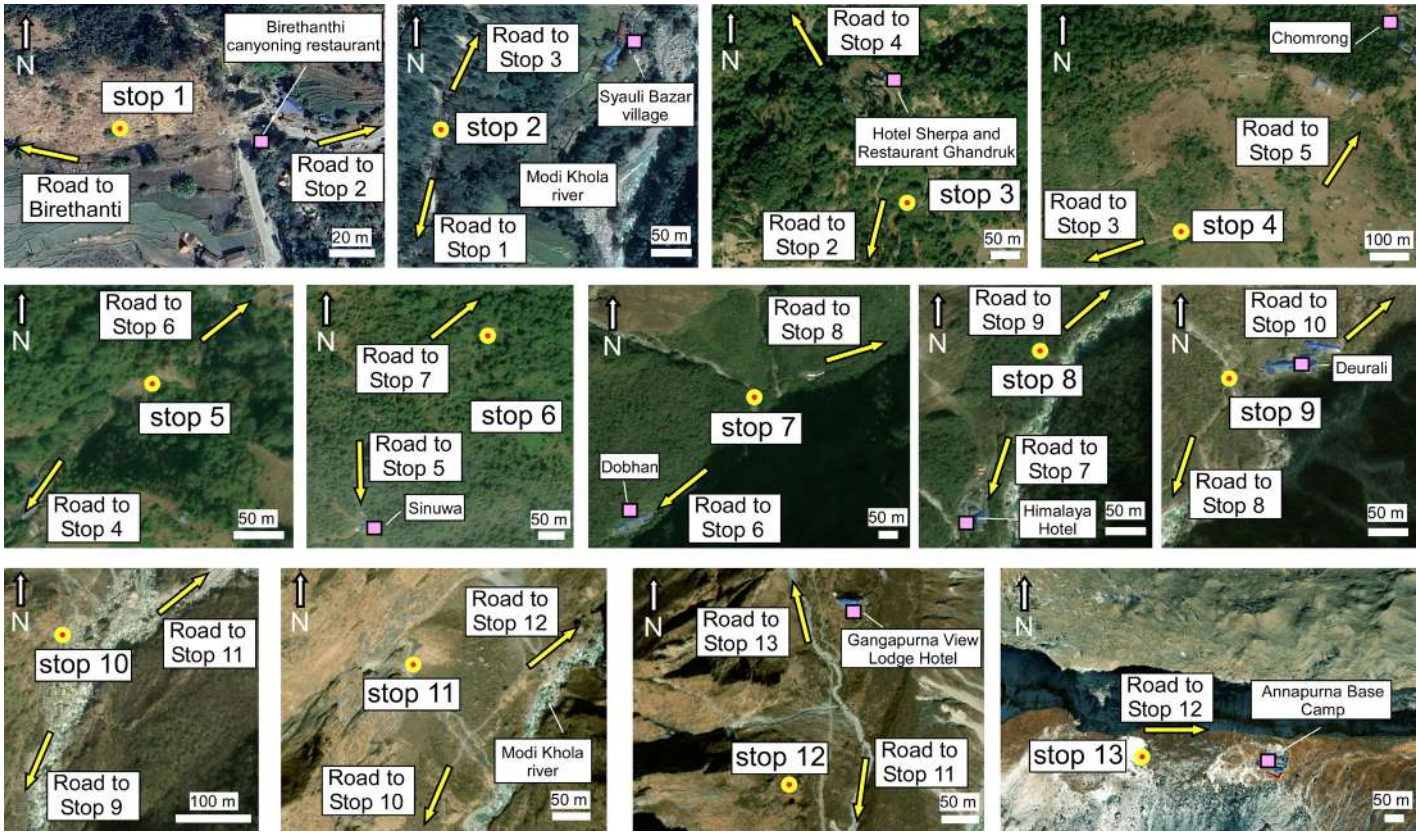

Fig. 7 - Location of the stops (1-13; yellow and red circle) on satellite images and their position with respect to the previous and following stop.

Stop 1 - Impure quarzites (LHS)

Coordinates: 28°19'09.0''N, 83°47'03.7''E, elevation 1088 m a.s.l.

The first stop (Figs. 1, 7) is located 3 km NE from the village of Birethanti (1500 m a.s.l.). This stop is representative of one of the constituents lithologies of the LHS. These are brownish impure quartzites that are foliated and fine grained (Fig. 8). The main foliation (S_{LHS}) strikes NW-SE and dips at medium-low angle towards NE.
In thin section the main foliation (S_{LHS}) is fine and continuous (Passchier and Trouw, 2005), predominantly defined by the iso-orientation of muscovite and biotite. The micas form 'bands' that sometimes anastomize around asymmetric aggregates of quartz crystals (Fig. 9) or around feldspars. It is possible to notice some kinematic indicators due to the deformation caused by the MCTZ. In addition, to further confirm and strengthen this, a sample of this outcrop has been analysed using the Universal Stage in order to obtain information about the preferred crystallographic orientation (CPO) of quartz.

Fig. 8 - Impure quartzites foliated and fine grained of the LHS at the outcrop-scale.

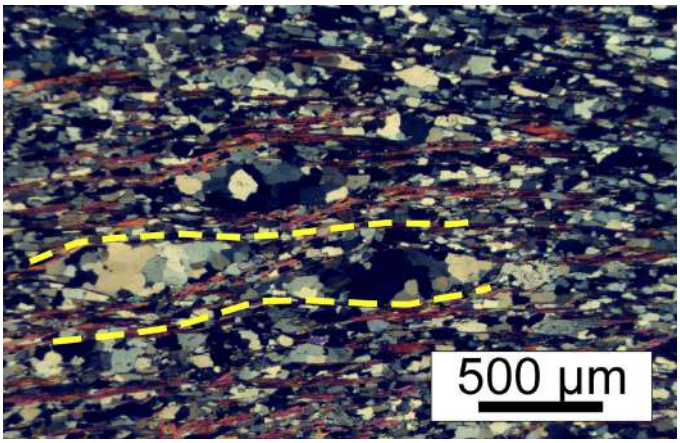

Fig. 9 - Main foliation S_{LHS} (yellow dashed lines) predominantly defined by the iso-orientation of muscovite and biotite that tend to anastomize around an asymmetric aggregate of quartz crystals (crossed nicols).

Stop 2 - Chlorite and sericite phyllites with blocks of quartzites (LHS)

Coordinates: 28°20'19.6''N, 83°47'58.5''E, elevation 1223 m a.s.l.

Chlorite and sericite phyllites locally with garnet are intercalated with the quartzites described in Stop 1. Stop 2 is representative of this other main lithology of the LHS (Figs. 1, 7). The outcrop is located at 1223 m a.s.l. halfway between the villages of Birethanti (1500 m a.s.l.) and Ghandruk (1993 m a.s.l.). At the outcrop-scale it is possible to see an evident S-C fabric pointing a top-to-the-S sense of shear (Fig. 10a), veins and boudinated quartz levels (Figs. 10b, c). Quartz in the phyllites also occurs in the form of asymmetric aggregates of sigmoidal shape also indicating a sense of shear top-to-the-S. The main foliation (S_{LHS}) is a crenulation cleavage (Fig. 10d), defined mostly by the iso-orientation and reorientation of micas (muscovite and biotite, the latter, sometimes being replaced by chlorite). As in the rest of the LHS the main foliation has a general strike NW-SE and dips at medium-low angle towards NE. Inside some microlithons is preserved a previous foliation (S^{-1}_{LHS}), fine and continuous defined by biotite and muscovite. In the domains richer in phyllosilicates, there is a further crenulation (S^{+1}_{LHS}; Fig. 10d) due to a third deformation phase.

Stop 3 - Ulleri Orthogneiss (LHS)

Coordinates: 28°22'19.9''N, 83°48'36.6''E, elevation 1859 m a.s.l.

Stop 3 is located just before the village of Ghandruk (1993 m a.s.l.), at an elevation of 1859 m a.s.l. (Figs. 1, 7). Here an outcrop of augen foliated and lineated mylonitic orthogneiss is present (Fig. 11). At the mesoscale kinematic indicators such as asymmetric feldspar porphyroclasts that indicate a sense of shear top-to-the-S are recognized (Fig. 11). This lithology is also known in literature as "Ulleri Orthogneiss" or "Ulleri Formation" or "Ulleri Auctt.". DeCelles et al. (2000), through U-Pb zircon dating, have provided protolith age of about 1831 Ma. The main foliation strikes NW-SE and dips at a medium angle towards NE. On the main foliation an object lineation defined by phyllosilicates and aggregates of quartz with a northward trend and shallow plunge. At the microscale the main foliation (S_{LHS}) is fine and disjunctive (Passchier and Trouw, 2005), characterized by cleavage domains, defined by phyllosilicates, which sometimes

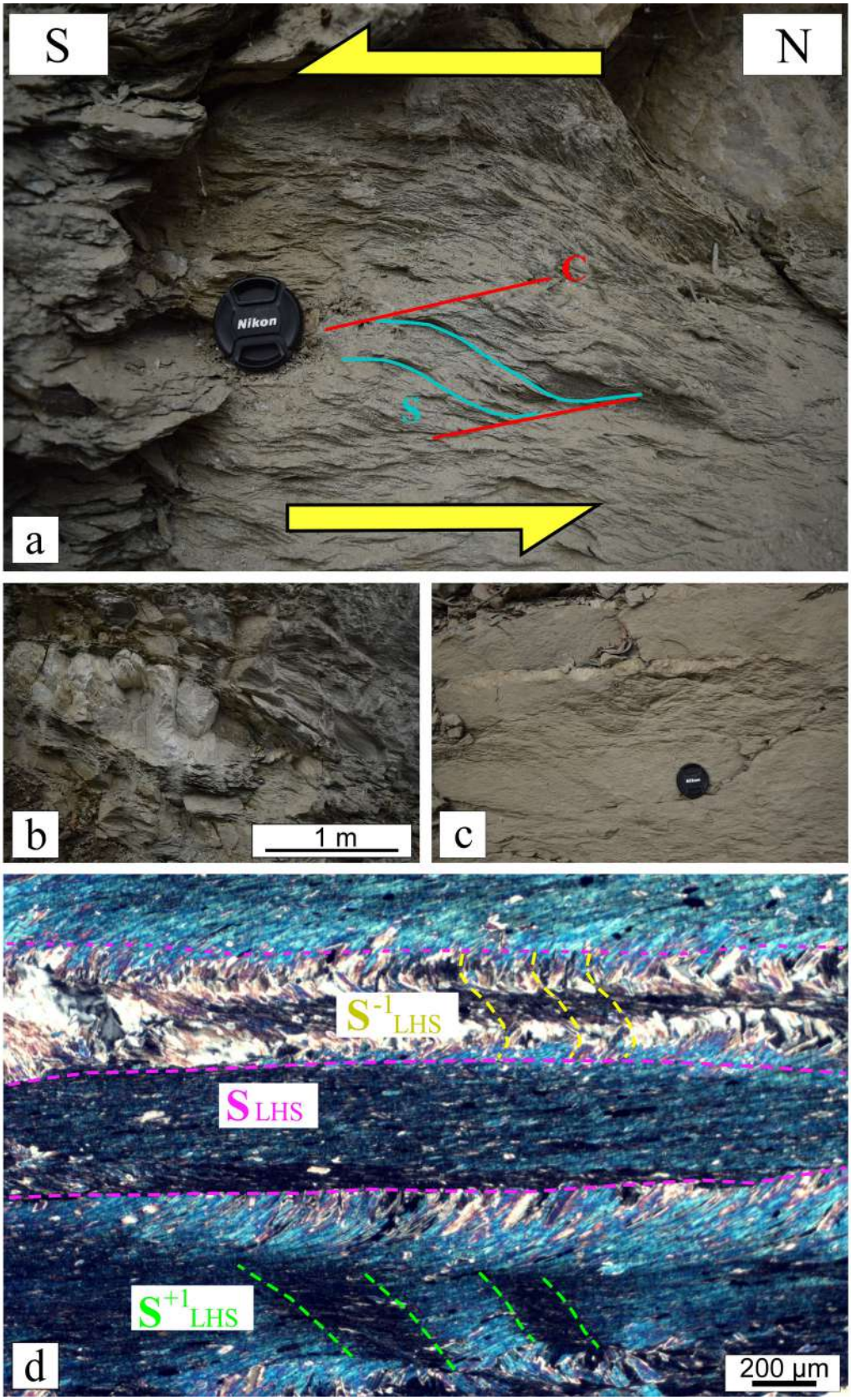

Fig. 10 - a. S-C fabric in phyllites pointing a top-to-the-S sense of shear at the outcrop-scale; b. Metric size boudinated quartz level in phyllites at the outcrop-scale; c. Boudinated quarz vein in phyllites; d. Thin section of a phyllite where three different foliations are recognizable: a main foliation S_{LHS} definable as a crenulation cleavage (highlighted by the pink dashed lines), a fine and continuous foliation, S^{-1}_{LHS}, preserved inside the microlithons (indicated by the yellow dashed lines) which tends to be reoriented according to the main foliation and a further crenulation S^{+1}_{LHS} in the domains richer in phyllosilicates (highlighted by the green dashed lines) (crossed nicols).

https://doi.org/10.3301/GFT.2025.03

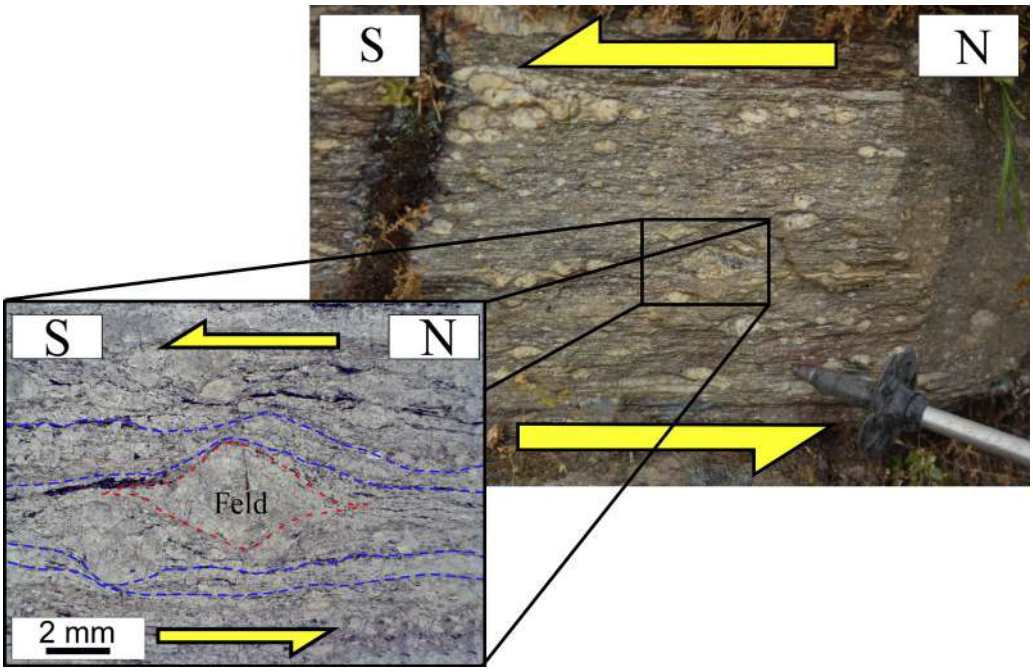

Fig. 11 - Augen foliated and lineated mylonitic orthogneiss at the outcrop-scale just S the village of Ghandruk (1993 m a.s.l.). The asymmetry of the feldspars indicates a top-to-the-S sense of shear; in thin section, an asymmetric rotated porphyroclast of feldspar (Feld; highlighted by the red dashed line). The blue dashed lines indicate the trend of the main foliation (S_{LHS}) (parallel nicols).

anastomize around porphyroclasts of feldspar (Fig. 11). Microlithons consist mostly of finely recrystallised quartz. Kinematic indicators such as σ type feldspars (Fig. 11), mica-fish type I, foliation fish and domino structures at the expense of feldspar are evident at the micro-scale.

Stop 4 - Quartzites (LHS)

Coordinates: 28°24'50.2''N, 83°48'44.7''E, elevation 2150 m a.s.l.

The stop number 4 (Figs. 1, 7) is located along the path between the river Kyumrun Khola and the village of Chomrong (2217 m a.s.l.). Here quartzites crop out (Fig. 12a). In this sector of the LHS, quartzites are alternated with methacarbonates and phyllites. The main foliation strikes NW-SE and dips moderately to NE (Fig. 12b). On the main foliation is recognizable an object lineation defined by phyllosilicates and quartz aggregates, plunging at medium-low angle (~30°) towards NE.

At the microscale for these quartzites is recognized a continuous foliation (Passchier and Trouw, 2005), materialized by the elongation of the phyllosilicates and the weak shape preferential orientation of quartz, which also presents a preferential crystallographic orientation. The foliation is also marked by a difference in the grain size. From the point of view of the quartz recrystallization mechanisms, irregular and lobed margins and wavy extinction typical of the Grain Boundary Migration (GBM) mechanism are observed (Fig. 12c). Given the proximity to the Upper MCT, in a sample of these quartzites, the orientation of c-axes of quartz was measured using the universal stage.

Stop 5 - Gneiss of Unit Ia (Lower GHS)

Coordinates: 28°25'38.6''N, 83°49'14.0''E, elevation 1924 m a.s.l.

The stop number 5 (Figs. 1, 7) is located along the trekking path between the villages of Chomrong (2217 a.s.l.) and Sinuwa (2330 m a.s.l.). Left behind us the rocks of the LHS, we are now in the rocks of the Lower GHS, in the Unit Ia, where paragneiss with garnet, locally migmatitic, crop out.

For the garnet, prograde zoning is described, and sometimes an increase in manganese content near the rim, which is indicative of resorption during the retrograde phase (Shrestha et al., 2020). From field observations, these rocks are fine grained and appear to be highly altered (Fig. 13). The main foliation in this area trends E-W and dips at a moderate to low angle towards N (~20°).

Because of the nature of this lithology there are no evident kinematic indicators either at the mesoscale or at the microscale, however, thanks to the abundance of quartz in these rocks located in the proximity of the BF, one of the cryptic discontinuities in the valley, the orientation of c-axis of quartz was measured for a sample collected from this outcrop.

A short distance to the N, within an outcrop of the same lithology, kinematic indicators were detected at the mesoscale in (Fig. 14).

Along the path that connects the villages of Sinuwa (2330 m a.s.l.) and Bamboo (2310 m a.s.l.) there is a very steep descent and is possible to see gneiss outcropping to the west.

https://doi.org/10.3301/GFT.2025.03

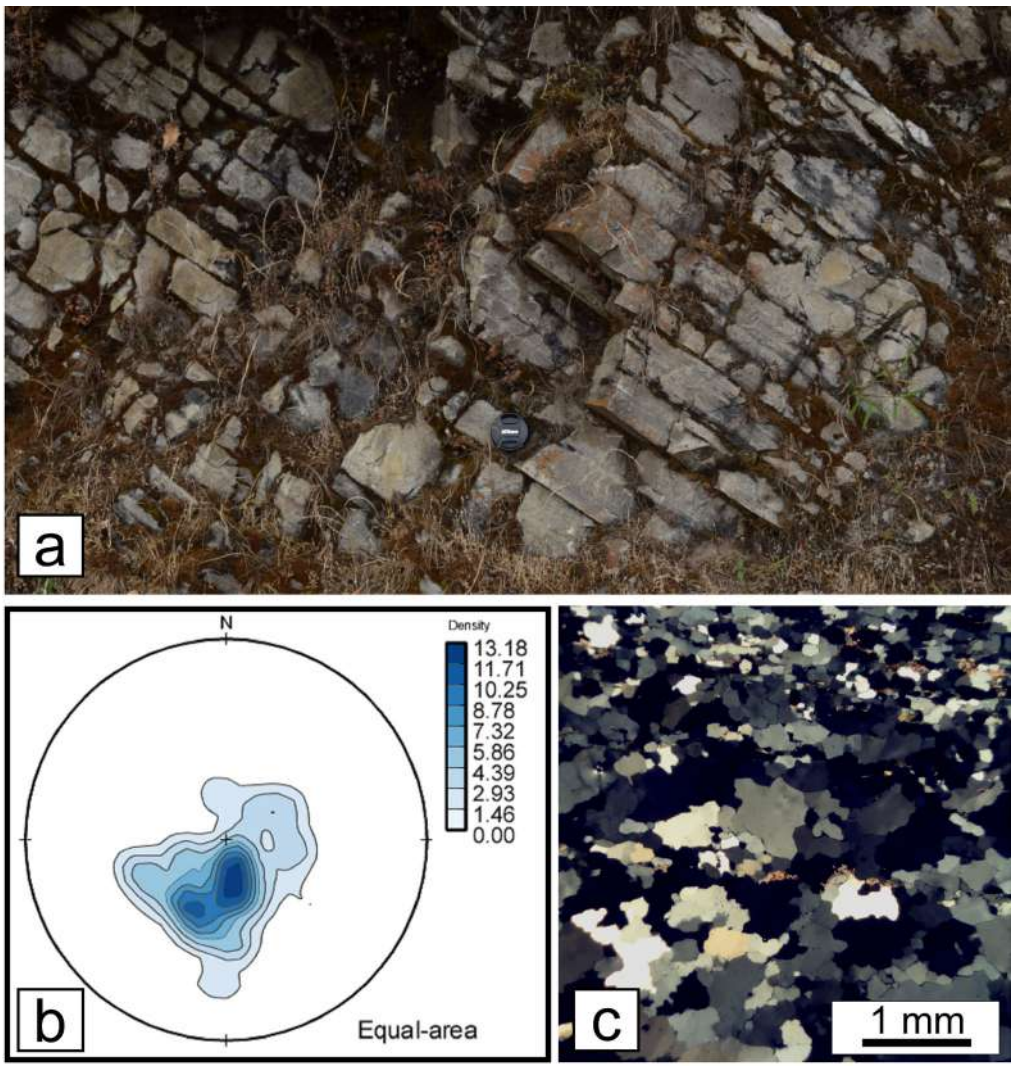

Fig. 12 - a. Quartzites of the LHS at outcrop-scale between the river Kyumrun Khola and the village of Chomrong (2217 m a.s.l.); b. Equal-area stereonet (lower hemisphere) showing the concentration of the main foliation poles in the LHS (62 measurements); the foliation has a general trend NW-SE and is dipping moderately to NE; c. Irregular and lobed margins and wavy extinction of quartz grains typical of the Grain Boundary Migration (GBM) recrystallization mechanism (crossed nicols).

Fig. 13 - Paragneiss with garnet, locally migmatitic, of the Unit Ia of the GHS at the outcrop-scale.

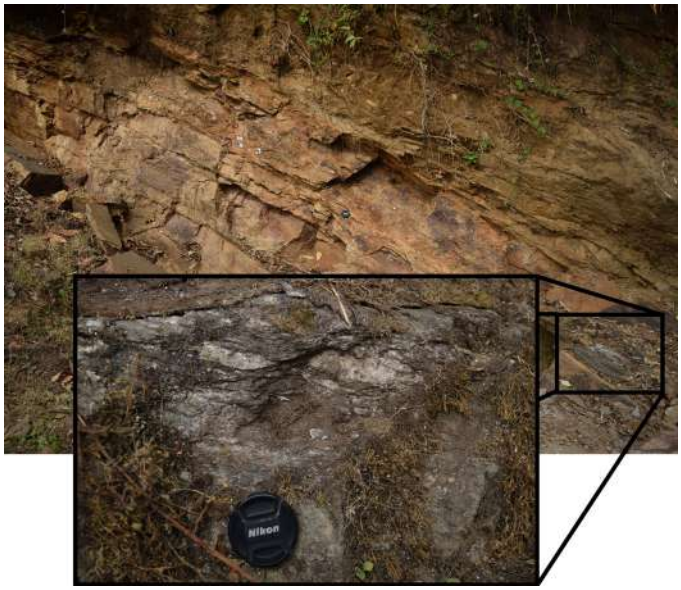

Fig. 14 - Shear-band boudin in the gneiss just before the village of Sinuwa (2330 m a.s.l.).

https://doi.org/10.3301/GFT.2025.03

Fig. 15 - Decimetric fold at the outcrop-scale in the gneiss of Unit Ib of the GHS showing a sense of transport toward the S.

Stop 6 - Decimetric fold in the gneiss of Unit Ib (Upper GHS)

Coordinates: 28°26'16.8''N, 83°50'27.0''E, elevation 2451 m a.s.l.

This stop is located at two-third way between the villages of Sinuwa (2330 m a.s.l.) and Bamboo (2310 m a.s.l.) and is representative of the first Unit of the Upper GHS, the Unit Ib (Figs. 1, 7). This unit differs from the previous one because it is almost entirely migmatic. The rocks of this unit are migmatitic paragneiss and garnet- and kyanite-bearing micaschists. The garnets are mostly homogeneous (Martin et al., 2010; Corrie and Kohn, 2011); sometimes an increase of manganese at the edges due to resorption during the retrograde phase has been observed (Shrestha et al., 2020).

In this stop it is possible to observe a decimetric fold in the gneiss (Fig. 15). The fold is closed, with rounded hinge and axial plane dipping at a low angle towards E-NE; there is no development of an axial plane foliation. The fold is likely associated with the deformation along the ST and the suggested sense of transport is toward the S.

For these rocks, at the microscale the main foliation (S_{GHS}) appears, depending on the case, continuous or spaced disjunctive (Passchier and Trouw, 2005), defined mostly by the iso-orientation of the phyllosilicates (biotite + muscovite). Foliation tends to be anastomosed around garnet porphyroclasts when present. Kinematic indicators, such as mineral-fish and foliation-fish (Fig. 16) are also present and those are pointing a top-to-the-S sense of shear (Fig. 16).

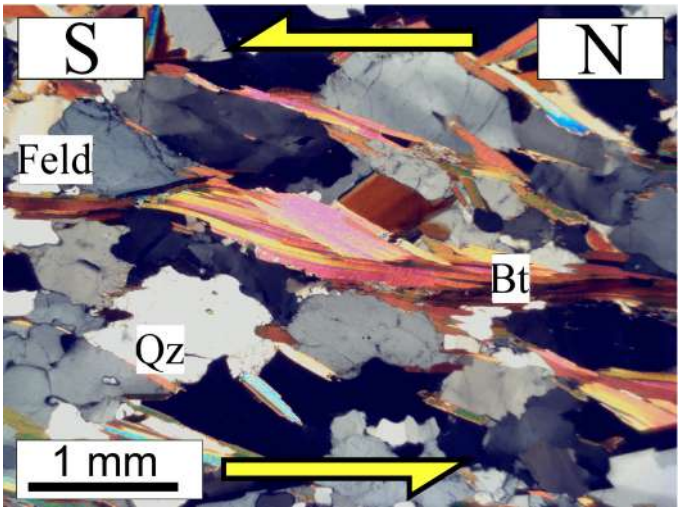

Fig. 16 - Foliation-fish showing a top-to-the-S sense of shear in the paragneiss of Unit Ib of the GHS (crossed nicols); Feld = feldspar, Qz = quartz, Bt = biotite (Whitney and Evans, 2010).

Stop 7 - Calcsilicatic gneiss of Unit II (Upper GHS)

Coordinates: 28°28'22.4''N, 83°52'23.1''E, elevation 2637 m a.s.l.

Structurally above the Units Ia and Ib, the Unit II consists of biotite- and hornblende-bearing gneiss, marbles and calcsilicatic gneiss crop out. The rocks of this Unit sampled in this area of study by Kohn and Corrie (2011) were used to estimate T-t respectively with the methods Zr-in-Ttn and U-Pb dating (700-750 °C at ~37 Ma; 775 °C at ~24 Ma; 765 °C at ~20 Ma).

The stop number 7 (Figs. 1, 7) is emblematic of this Unit and is located in correspondence of a stream, north of the village of Dobhan (2735 m a.s.l.). It is possible to observe

banded calcsilicatic gneiss with leucogranitic intrusions parallel to the foliation or that cut it (Figs. 17a, b), locally boudinated around large crystals of tourmaline (Figs. 17b, c). The main foliation trends E-W and dips at a medium angle towards N.
At the microscale those rocks present a main foliation (S_{GHS}) that tend to be anastomosed around garnet phorphyroclasts when present (Fig. 17d).

Stop 8 - Migmatitic orthogneiss of Unit III (Upper GHS)

Coordinates: 28°29'11.7''N, 83°53'22.3''E, elevation 2883 m a.s.l

The stop number 8 (Figs. 1, 7) is located between the locality of Himalaya Hotel (2853 m a.s.l.) and the village of Deurali (3164 m a.s.l.). This outcrop is representative of the Unit III of the Upper GHS. The lithology is a migmatitic orthogneiss (Fig. 18a) with visible centimetric porphyroclasts of feldspar (Fig. 18b). At the outcrop-scale it is worth noting that the feldspars appear to be fractured, index of low-medium grade conditions (400 – 500 °C; Passchier and Trouw, 2005). The protolith of this lithology has been dated to about 500 Ma with the zircon U-Pb dating method by Hodges et al. (1996). The biotite- and garnet-bearing gneiss, sometimes migmatitic, also belong to the Unit III of the GHS. The garnets of these rocks are homogeneous with an increase of manganese at the edges, indicating first HT conditions and subsequent resorption during the retrograde phase (Corrie and Kohn, 2011; Shrestha et al., 2020). The sillimanite described in these rocks has been interpreted as metasomatic and not as primary (Corrie and Kohn, 2011).
In this lithology, consistent with the overall trend observed in the GHS, the foliation displays a prevalent NW- SE orientation, with a moderate to low dip angle towards NE.
Along the Mardi Himal trek, parallel to the Modi Khola valley,

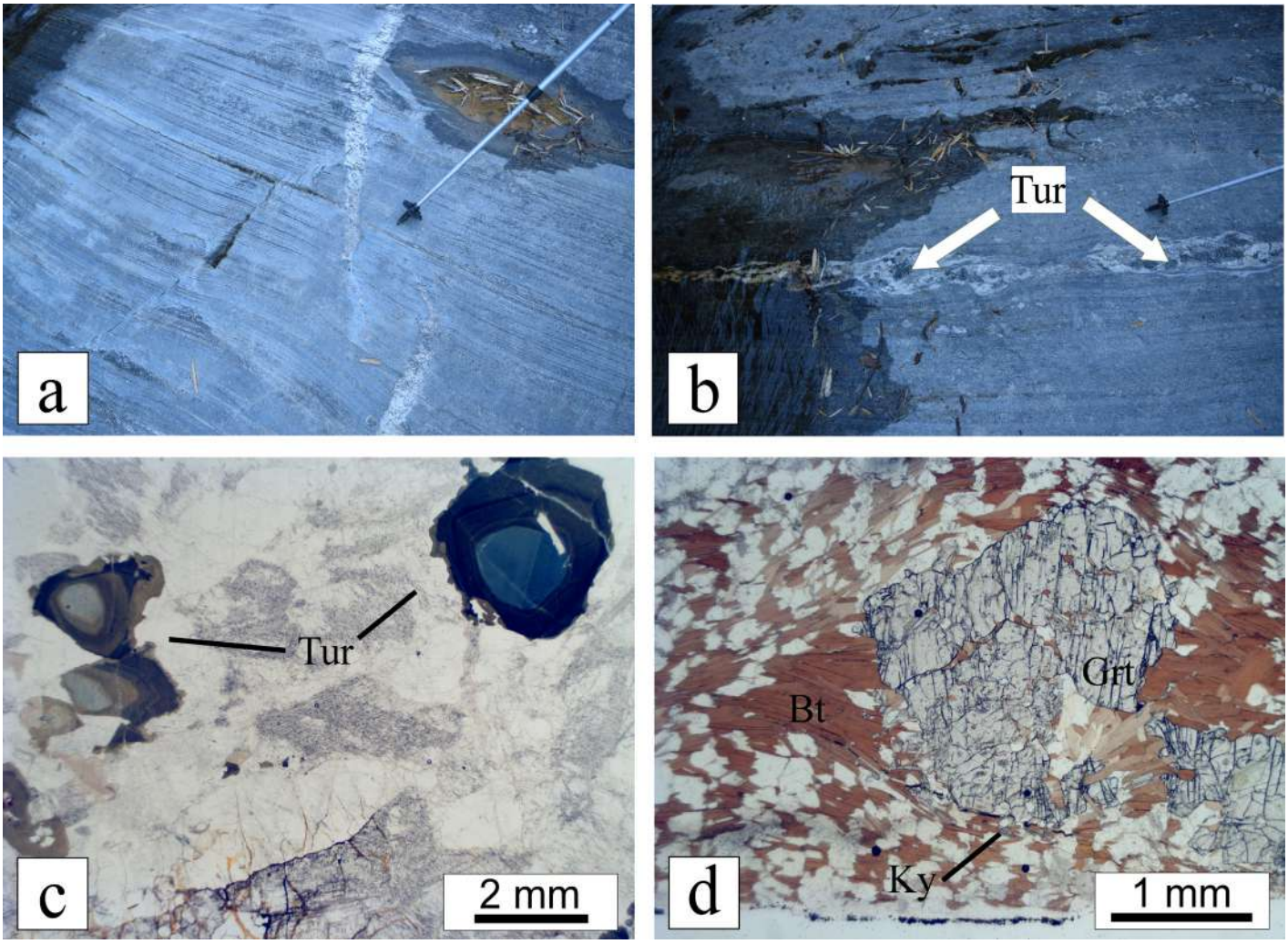

Fig. 17 - a. Leucogranitic intrusion that cut the foliation and form a bridge in the calcsilicatic gneiss; b. Boudinated leucogranitic intrusion parallel to the foliation in the calcsilicatic gneiss in which are recognizable centimetric tourmaline crystals (dark colour); c. Millimetric zoned basal sections of tourmaline (parallel nicols); d. Main foliation (S_{GHS}) that anastomize around a millimetric garnet phorphyroclast (parallel nicols). Tur = tourmaline, Bt = biotite, Ky = kyanite, Grt = garnet (Whitney and Evans, 2010).

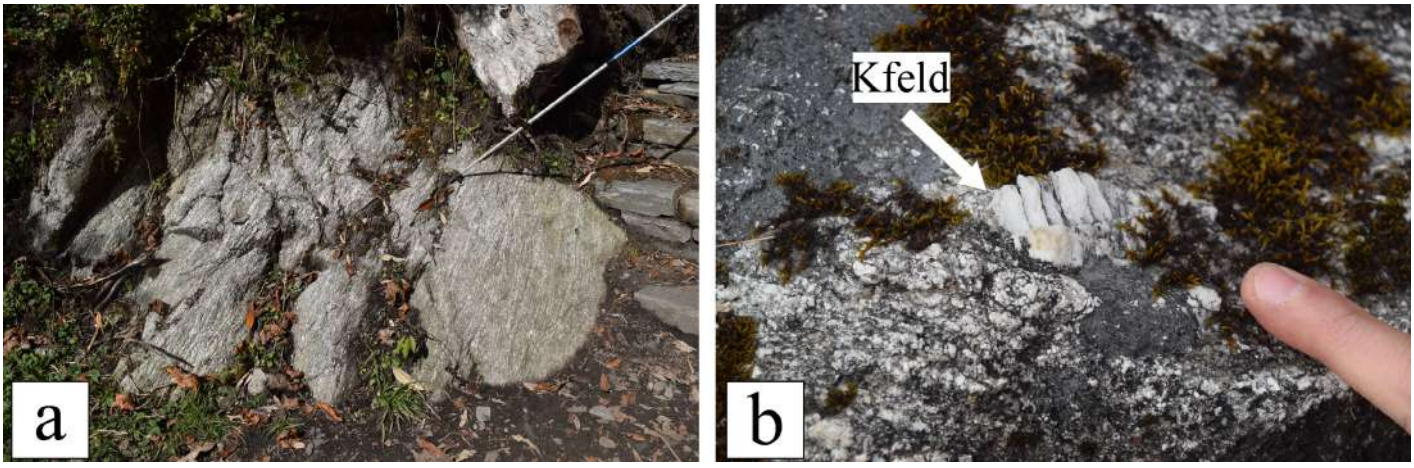

Fig. 18 - a. Migmatitic orthogneiss of Unit III of the GHS outcropping between the locality of Himalaya Hotel (2853 m a.s.l.) and the village of Deurali (3164 m a.s.l.); b. Fractured centimetric porphyroclast of feldspar (Kfeld) in the migmatitic orthogneiss of Unit III of the GHS.

the rocks of this unit are better exposed at the outcrop-scale and locally show leucogranitic intrusions transposed and parallelized to the main foliation (S_{GHS}; Fig. 19).

Stop 9 - Calcsilicatic gneiss of Unit IV (Upper GHS)

Coordinates: 28°29'49.6''N, 83°53'49.6''E, elevation 3033 m a.s.l.

The stop number 9 (Figs. 1, 7) is representative of the structurally upper part of the GHS. Unit IV is characterized by marbles and calcsilicatic gneiss with biotite (Fig. 20a). This unit differs from Unit II of the GHS due to the presence of locally boudinated leucogranitic intrusions with muscovite and tourmaline (Fig. 20b). The stop is located before the village of Deurali (3164 m a.s.l.) and here is possible to observe calcsilicatic gneiss with significant-sized pyroxene (Diopside) and hornblende porphyroclasts (Fig. 20c). In thin section, the pyroxene crystals exhibit skeletal and relict textures (Fig. 20c).

Fig. 19 - Migmatitic orthogneiss with evident transposed intrusions parallel to the main foliation (S_{GHS}), located slightly N of the Base Camp along the Mardi Himal trek.

The main foliation strikes NW-SE and dips at medium angle towards NE.

The abundant leucogranitic intrusions are prominently visible in the panorama (Fig. 21a) and can be traced from below the peak of Mardi Himal (5553 m a.s.l.; Fig. 21b) to beneath the peak of Hiunchuli (6441 m a.s.l.; Fig. 21c), located west of the Modi Khola Valley. The intrusions exhibit boudinage parallel to the main foliation and are locally bifurcated. The boudins display both symmetric and asymmetric characteristics. The originally high-angle intruding veins are often affected by asymmetric folding (Fig. 21d). Deformed intrusions cutting across the main foliation are also documented. The rocks of Unit IV of the GHS are separated from the overlying rocks of the THS by the Mardi-Himal Detachment, with the latter rarely exhibiting such intrusions in the lower portion near the contact.

Stop 10 - Modi Khola Shear Zone evidence in the Unit IV (Upper GHS)

Coordinates: 28°30'06.1''N, 83°54'03.5''E, elevation 3158 m a.s.l.

In the Modi Khola valley, the structurally highest part of the GHS (Unit IV) is affected by a significant ductile shear zone called the Modi Khola Shear Zone. Stop number 10 (Figs. 1, 7), located close to the village of Deurali (3164 m a.s.l.), is crucial as it allows the observation of outcrop-scale evidence of this shear zone. In this point of the trek is possible to observe clear and evident kinematic indicators (Fig. 22) such as asymmetric centimetre-sized porphyroclasts, both of σ type and δ type, as well as other indicators like flanking-folds. Porphyroclasts of the φ type are also present.

https://doi.org/10.3301/GFT.2025.03

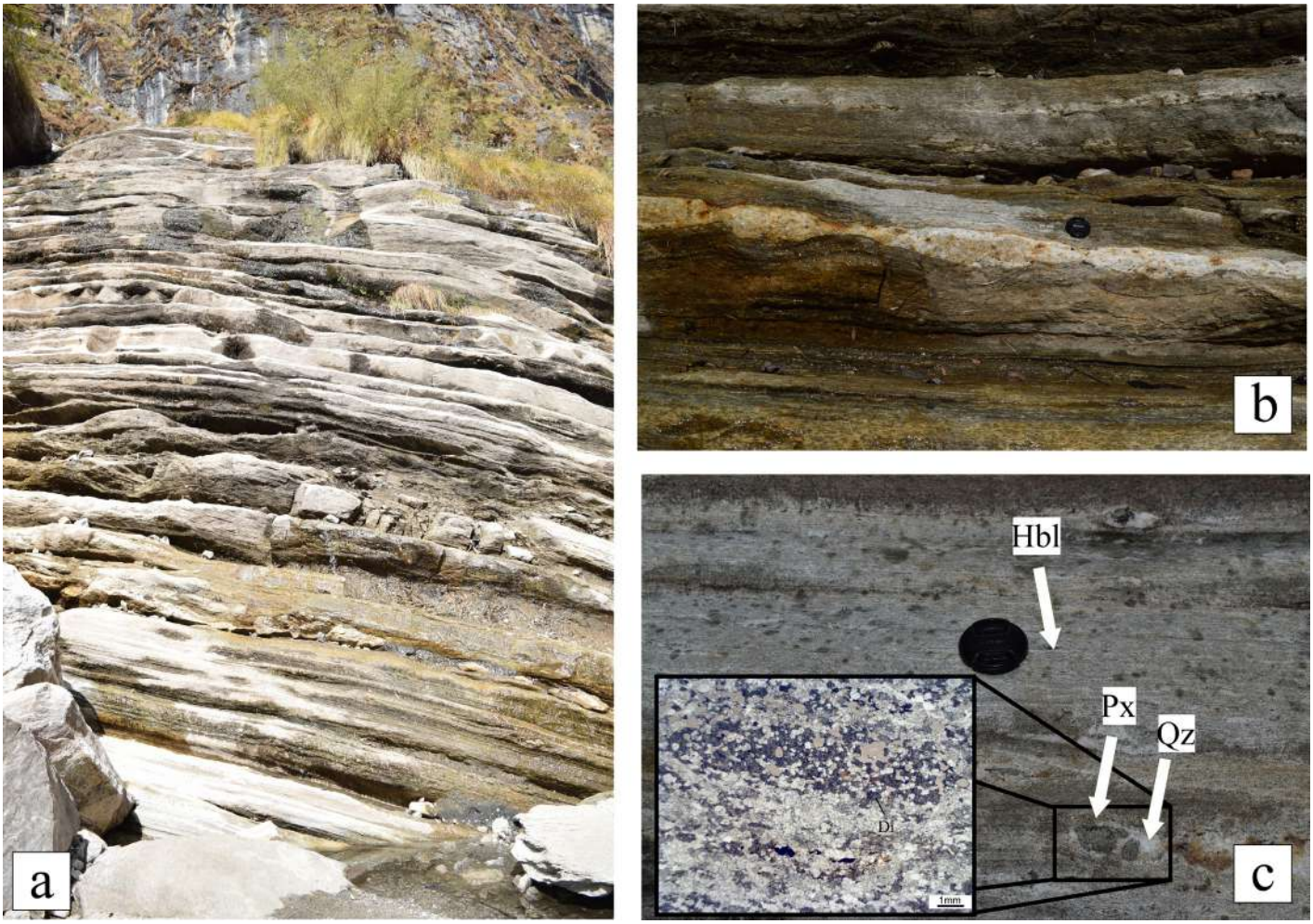

Fig. 20 - a. Calcsilicatic gneiss of Unit IV of the GHS outcropping slightly before the village of Deurali (3164 m a.s.l.); b. Boudinated leucogranitic intrusion with muscovite and tourmaline within the calcsilicatic gneiss of Unit IV of the GHS; c. Porphyroclasts, of considerable size, of pyroxene (green in colour), surrounded by portions rich in quartz in the calcsilicatic gneiss of Unit IV; there is also hornblende, dark in colour, almost black. In thin section, a millimetric skeletal pyroxene crystal (parallel nicols); Hbl = hornblende, Px = pyroxene, Qz = quartz, Di = diopside (Whitney and Evans, 2010).

These kinematic indicators suggest a top-to-the-S sense of shear. The foliation measured in outcrops affected by the MKSZ has a consistent orientation with that measured in other lithologies belonging to the GHS. The foliation trends NW-SE and dips at a low angle (~30°) towards E-NE (Fig. 23). On the foliation, where visible, a lineation with a trend towards E-NE and plunging at moderately low angle (~30°) has been measured (Fig. 23). Hodges et al. (1996) consider the MKSZ as an out-of-sequence thrust active between 22.5 and 18.5 Ma (U-Pb dating on monazite, zircon and xenotime in deformed leucogranites). More recently, Kohn and Corrie (2011) obtained T-t estimates using the Zr-in-Ttn and U-Pb dating methods for two samples of calcsilicatic rocks from Unit IV of the GHS.

Specifically, one of the aforementioned samples, located near the MKSZ, provided temperature values of approximately 700 °C at around 37 Ma, approximately 775 °C at around 24 Ma, and around 765 °C at 21 Ma (Fig. 24). However, Kohn and Corrie (2011) do not directly attribute these T-t estimates to the activity of the MKSZ but instead utilize this data for a broader-scale reconstruction of the exhumation mechanisms of the GHS. In the future, an important contribution could be provided by a detailed geochronological study aimed at precisely constraining the age of deformation along the MKSZ.

Stop 11 - Annapurna Yellow Formation (THS)

Coordinates: 28°30'43.1''N, 83°54'15.4''E, elevation 3414 m a.s.l.

Moving away from the rocks of the GHS behind us, stop number 11 is located within the rocks of the THS, most precisely in the Annapurna Yellow Formation (Figs. 1, 7). This stop is located between the village of Deurali (3164 m a.s.l.) and the Machapuchare Base Camp (3700 m a.s.l.). In the Modi Khola valley, according to Hodges et al. (1996), the rocks of the Annapurna Yellow Formation, crop out below

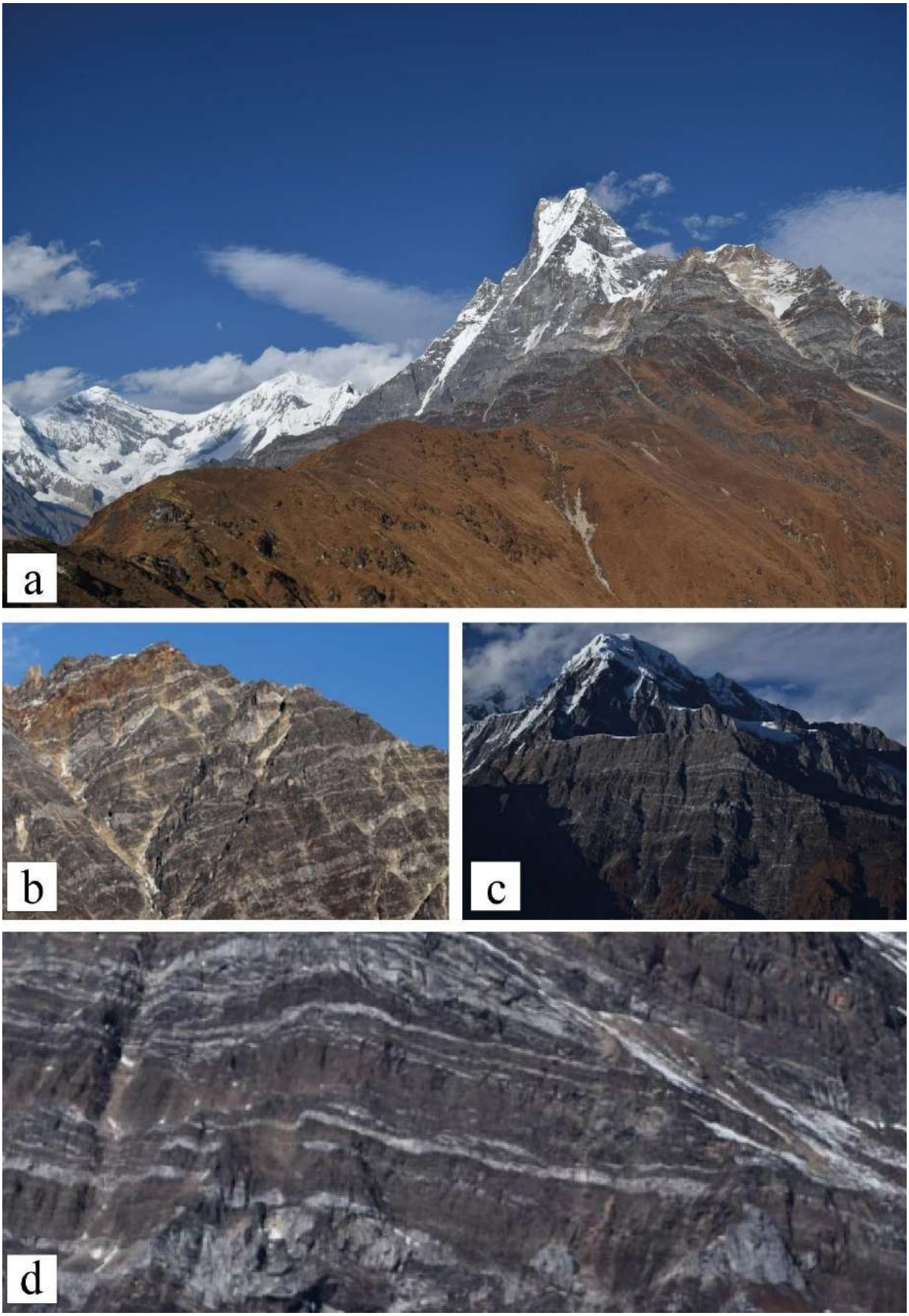

Fig. 21 - a. Panoramic view towards N-NW of Mardi Himal (5553 m a.s.l.) in the foreground on the right with Machapuchare (6993 m a.s.l.) behind; the valley on the left is the Modi Khola. In the grey portion, leucogranitic intrusions are visible; b. Detail of leucogranitic intrusions below the peak of Mardi Himal (5553 m a.s.l.); c. Leucogranite intrusions below the peak of Hiunchuli (6441 m a.s.l.); d. Boudinated and folded intrusions below the summit of Hiunchuli (6441 m a.s.l.).

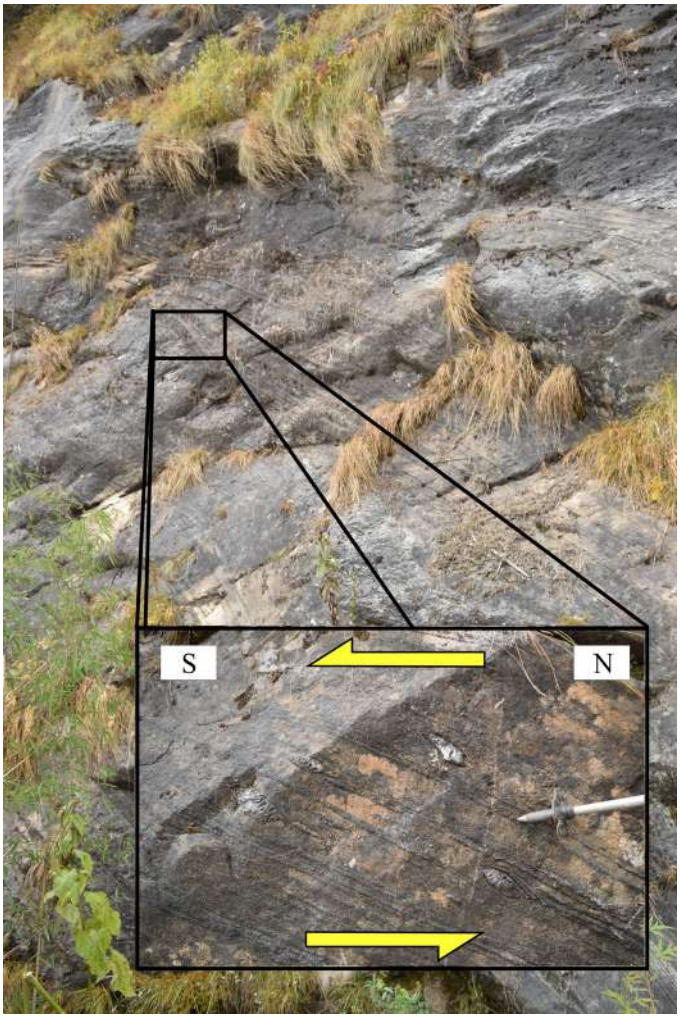

Fig. 22 - Kinematic indicators, at the outcrop- scale, in the calcsilicatic gneiss of Unit IV of the GHS related to the activity along the MKSZ pointing a top-to-the-S sense of shear.

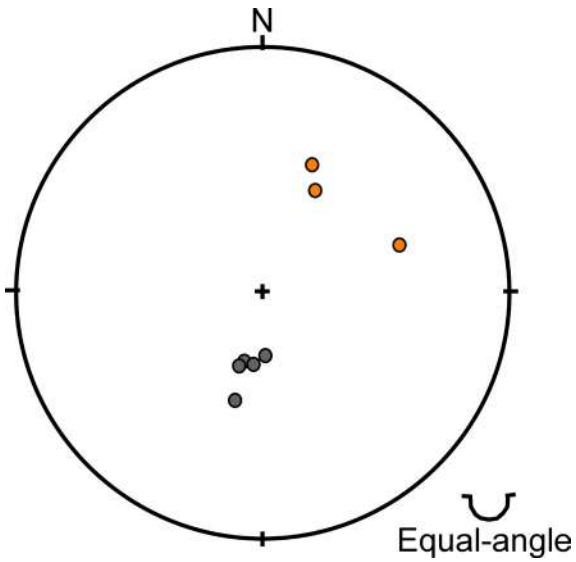

Fig. 23 - Equal-area projection, lower hemisphere. The black dots (n: 5) represent the poles of the main foliation (S_{GHS}) near the MKSZ, while the orange dots (n: 3) show the lineation.

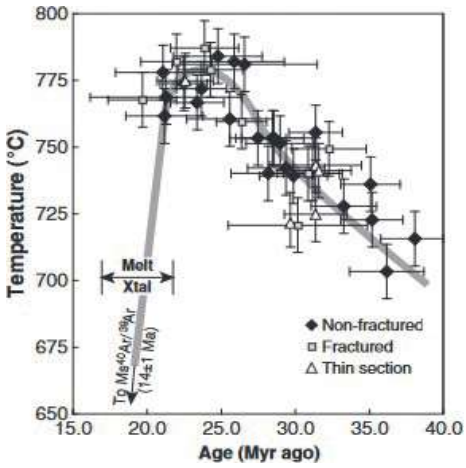

Fig. 24 - Temperature time history (grey lines) for GHS calcsilicatic gneiss on a sample collected close to the MKSZ. Approximate obtained values: ~700 °C at around 37 Ma, ~775 °C at around 24 Ma, and ~765 °C at 21 Ma (modified from Kohn and Corrie, 2011).

the rocks of the Sanctuary Formation. Here, in the outcrop, it is possible to observe the marbles of the mentioned formation. Leucogranitic intrusions affected by asymmetric folds can be observed (Fig. 25a). The same intrusions are boudinated (Fig. 25b) and later folded (Fig. 25c) and this represents an evidence of a complex polyphase deformation in the area. The main foliation strikes NW-SE and dips at moderate angle towards NE. An object lineation defined by the biotite and plunging at moderate angle towards NE has been measured.

Locally, on the main foliation, a static recrystallization of amphibole forming radiating aggregates has been observed. In thin section, a dominant anisotropy (S_{THS}) can be recognized, primarily defined by the preferred shape orientation of calcite (Fig. 25d) and to a lesser extent by the iso-orientation of phyllosilicates. In terms of recrystallization mechanisms, calcite exhibits both type I and type II twins (Fig. 25e), and triple junctions between grains are occasionally observed, indicating partial annealing phenomenon (Fig. 25e).

Stop 12 - Sanctuary Formation (THS)

Coordinates: 28°31'18.1''N, 83°54'27.4''E, elevation 3683 m a.s.l.

Stop 12 (Figs. 1, 7) is representative of the other lithology that makes up the THS in the Modi Khola Valley. At this stop, located just before the Machapuchare Base Camp (3700 m a.s.l.), it is possible to observe an outcrop of altered impure quartzites of the Sanctuary Formation (Fig. 26a). The Sanctuary Formation and the Annapurna Yellow Formation are affected by multi-kilometric folds that complicate their structural arrangement; in particular this relationship can

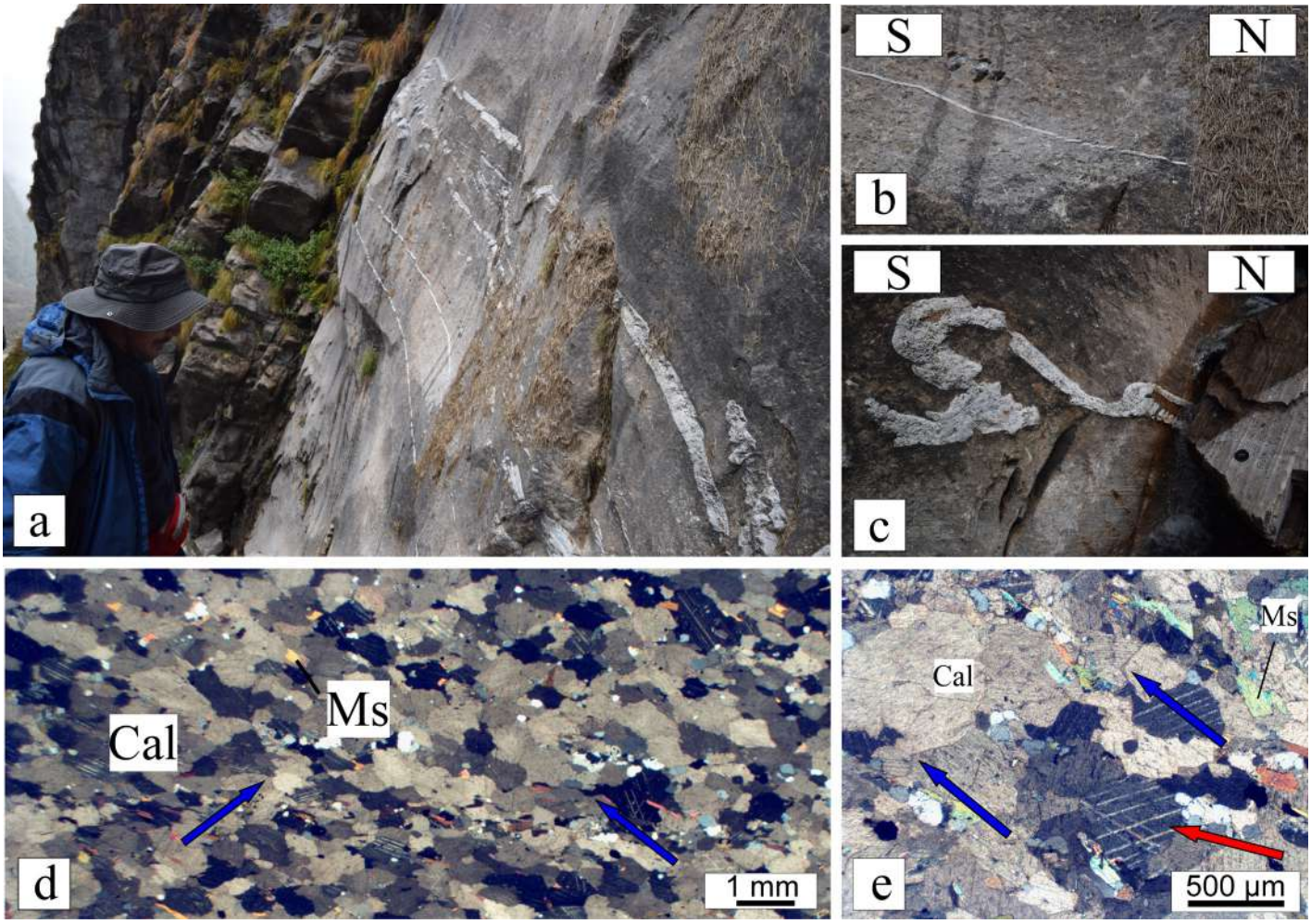

Fig. 25 - a. Marbles of the Annapurna Yellow Formation (THS) with boudinated and folded intrusions, outcropping between the village of Deurali (3164 m a.s.l.) and the Machapuchare Base Camp (3700 m a.s.l.); b. Detail of a domino-boudin in the marbles of the Annapurna Yellow Formation; c. Detail of asymmetric folded intrusion in the marbles of the Annapurna Yellow Formation; d. Thin section showing the main anisotropy (S_{THS}) given by the preferential shape orientation of the calcite and to a lesser extent by the iso-orientation of the phyllosilicates; the blue arrows indicate the irregular edges of the calcite, due to the possible dynamic recrystallization by the Grain Boundary Migration (GBM) mechanism (crossed nicols); e. Type II mechanical twinnings in calcite (red arrow) and triple joints at calcite grain boundaries (blue arrows), due to partial annealing (crossed nicols). Cal = calcite; Ms = muscovite (Whitney and Evans, 2010).

be observed in greater detail at stop 13 on a larger scale. At the metric and decametric scale, in this outcrop the relationships between two folding phases can be observed (Figs. 26a, b), resulting in a type III interference pattern (Ramsay et al., 2002). In a sector further west, Colchen et al. (1986) highlight how the Sanctuary Formation is the nucleus of a large-scale anticline fold (with a width of more than 5 km). In the Modi Khola valley it is possible to observe the reverse flank of this structure, occupied by the Sanctuary Formation (Hodges et al., 1996). At the outcrop scale a main foliation trending ~E-W and dipping at moderate angle toward N has been measured. In thin section, the main foliation (S_{THS}) is generally fine and continuous, primarily defined by the iso-orientation of phyllosilicates (biotite and ± muscovite ± chlorite) and sometimes by the preferred shape orientation of quartz and/or calcite aggregates.

Stop 13 - Machapuchare Fold (THS)

Coordinates: 28°31'51.2"N, 83°52'28.3"E, elevation 4130 m a.s.l.

Stop 13 (Figs. 1, 7) is a panoramic stop located just west of the Annapurna Base Camp (4130 m a.s.l.). This stop is crucial for understanding the relationships between the Sanctuary Formation and the Annapurna Yellow Formation. Colchen et al. (1986) mapped in the area a ~E-W trending kilometric-scale antiformal syncline, the "Fang nappe", related to a deformational phase 1 and responsible of the stratigraphic inversion of the THS rocks in the hanging-wall of the detachment (Hodges et. al., 1996).

On the western side of Mount Machapuchare (6993 m a.s.l.), a recumbent syncline that refold the "Fang nappe" and related to a deformational phase 2, can be observed

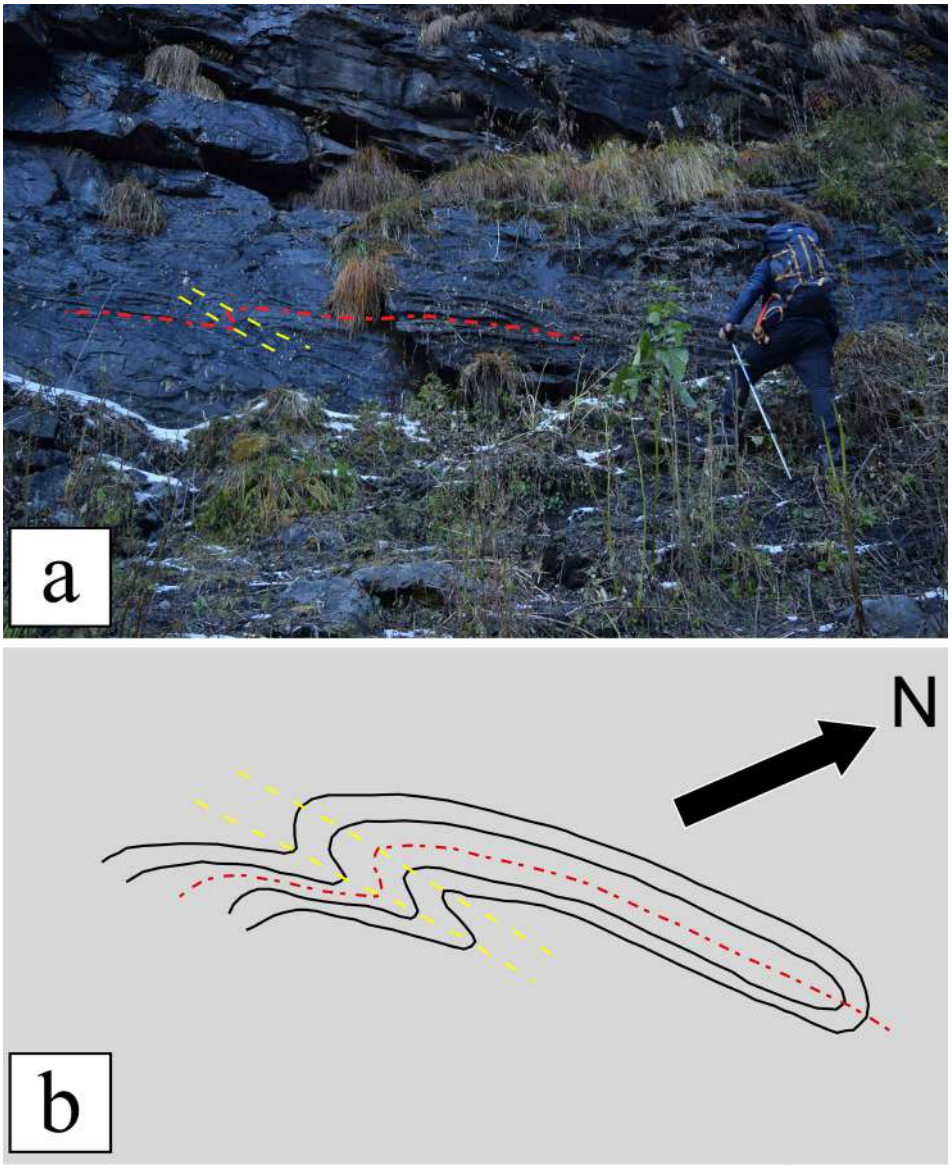

Fig. 26 - a. Sanctuary Formation outcrop S of Machapuchare Base Camp (3700 m a.s.l.); type III interference given by two plicative phases is recognizable. The axial plane of the oldest fold is indicated in dashed red while the axial planes of the next phase are shown in yellow; b. Schematic sketch of the structure of Fig. 26a.

(highlighted by the yellow dashed lines; Figs. 27, 28), affecting the lithologies of the Sanctuary Formation and the Annapurna Yellow Formation (forming the core of the fold). Below, the Hiunchuli-Machapuchare Detachment is visible (shown in red; Fig. 27), and on the left, there is an associated splay of the detachment.

ACKNOWLEDGMENTS

This work is part of a master's thesis, which in turn is a component of the PRIN 2015 national research project titled "The subduction and exhumation of the continental lithosphere: their effects on the structure and evolution of the orogens.", for which I express my gratitude to Montomoli Chiara and Carosi Rodolfo (Earth Sciences Department, University of Turin). Furthermore, the research project received co-financing from the Ministry of Education, Universities, and Research (MUR) for the Earth Sciences Department of the University of Turin for whose contributions I extend my appreciation to Iaccarino Salvatore (Earth Sciences Department, University of Turin). Additionally, it received partial support from the European Union through an extra-Erasmus call. The project also represents an ongoing collaboration between the Earth Sciences Department of Turin, Italy, and the Central Department of Geology of Tribhuvan University in Kathmandu, Nepal.
In conclusion, I would like to extend my heartfelt gratitude to Chiara and Salvatore for their unwavering support and guidance throughout my thesis journey.

Fig. 27 - Panoramic view from the Annapurna Base Camp (4130 m a.s.l.) in which a clearly evident synclinal fold can be observed on the west side of Mount Machapuchare (6993 m a.s.l.), which affects the lithologies of the Sanctuary Formation and the Annapurna Yellow Formation (dashed yellow lines), and below, in red, the Hiunchuli-Machapuchare Detachment; on the left, in red, a splay of the latter.

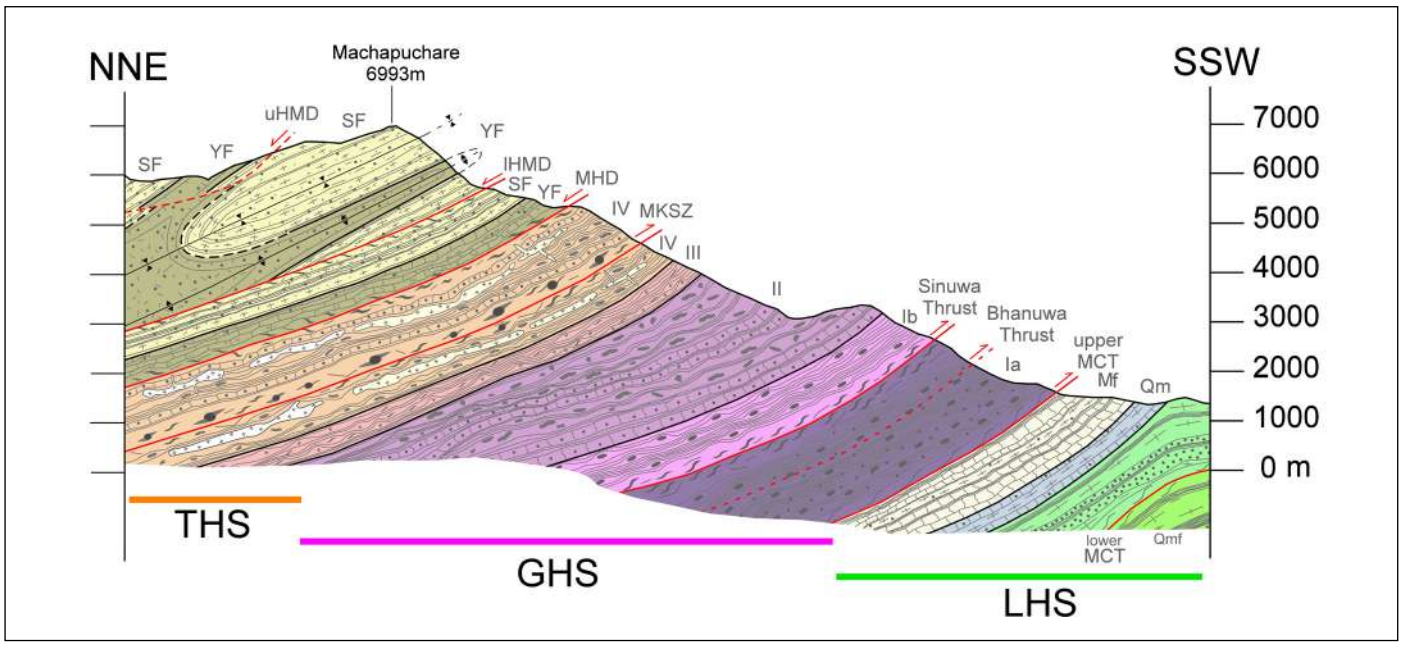

Fig. 28 - Geological cross-section of part of the lithologies present in the Modi Khola valley and of the main structures. Qmf: Quartzites, metapelites and phillites; Qm: Quartzites and marbles; Mf: Metacarbonates and phillites; YF: Annapurna Yellow Formation; SF: Sanctuary Formation; MCT: Main Central Thrust; MKSZ: Modi Khola Shear Zone; MHD: Mardi-Himal Detachment; HMD: Hiunchuli- Machapuchare Detachment; LHS: Lesser Himalayan Sequence; GHS: Greater Himalayan Sequence; THS: Tethyan Himalayan Sequence.

REFERENCES

Ader T., Avouac J.-P., Liu-Zeng J., Lyon-Caen H., Bollinger L., Galetzka J., Genrich J., Thomas M., Chanard K., Sapkota S.N., Rajaure S., Shrestha P., Ding L., Flouzat M. (2012) - Convergence rate across the Nepal Himalaya and interseismic coupling on the Main Himalayan Thrust: Implications for seismic hazard. J. Geophys. Res.: Solid Earth, 117, B04403, https://doi.org/10.1029/2011JB009071.

Antolín B., Appel E., Montomoli C., Dunkl I., Ding L., Gloaguen R., El Bay R. (2011) - Kinematic evolution of the eastern Tethyan Himalaya: constraints from magnetic fabric and structural properties of the Triassic flysch in SE Tibet. Geol. Soc. Spec. Publ., 349(1), 99-121, https://doi.org/10.1144/SP349.6.

Beaumont C., Jamieson R.A., Nguyen M.H., Lee B. (2001) - Himalayan tectonics explained by extrusion of a low-viscosity crustal channel coupled to focused surface denudation. Nature, 414(6865), 738-742, https://doi.org/10.1038/414738a.

Bilham R., Larson K., Freymueller J. (1997) - GPS measurements of present-day convergence across the Nepal Himalaya. Nature, 386(6620), 61-64, 10.1038/386061a0.

Carosi R., Montomoli C., Iaccarino S. (2018) - 20 years of geological mapping of the metamorphic core across Central and Eastern Himalayas. Earth Sci Rev., 177, 124-138, https://doi.org/10.1016/j.earscirev.2017.11.006.

Colchen M., Le Fort P., Pêcher A. (1986) - Recherches géologiques dans l'Himalaya du Népal: Annapurna-Manaslu- Ganesh Himal = Geological researches in the Nepal's Himalaya: Annapurna-Manaslu-Ganesh Himal. 136 pp. Editions du Centre national de la recherche scientifique: Diffusion, Presses du CNRS, Paris.

Copley A., Avouac J.-P., Royer J.-Y. (2010) - India–Asia collision and the Cenozoic slowdown of the Indian plate: Implications for the forces driving plate motions. J. Geophys. Res.: Solid Earth, 115, B03410, https://doi.org/10.1029/2009JB006634.

Corrie S.L., Kohn M.J. (2011) - Metamorphic history of the central Himalaya, Annapurna region, Nepal, and implications for tectonic models. Geol. Soc. Am. Bull., 123(9-10), 1863-1879, https://doi.org/10.1130/B30376.1.

Crouzet C., Dunkl I., Paudel L., Árkai P., Rainer T.M., Balogh K., Appel E. (2007) - Temperature and age constraints on the metamorphism of the Tethyan Himalaya in Central Nepal: A multidisciplinary approach. J. Asian Earth Sci., 30(1), 113-130, https://doi.org/10.1016/j.jseaes.2006.07.014.

Decelles P.G., Gehrels G.E., Quade J., LA Reau B., Spurlin, M. (2000) - Tectonic Implications of U-Pb Zircon Ages of the Himalayan Orogenic Belt in Nepal. Science, 288(5465), 497-499, 10.1126/science.288.5465.497.

Dèzes P. (1999) - Tectonic and Metamorphic Evolution of the Central Himalayan Domain in Southeast Zanskar (Kashmir, India). Mémoires de Géologie (Lausanne), 32, 145 p.

Doglioni C., Panza G. (2015) - Polarized Plate Tectonics. Advances in Geophysics. Elsevier, 1-167, https://doi.org/10.1016/bs.agph.2014.12.001.

Doglioni C., Carminati E., Cuffaro M., Scrocca, D. (2007) - Subduction kinematics and dynamic constraints. Earth Sci Rev., 83(3-4), 125-175, https://doi.org/10.1016/j.earscirev.2007.04.001.

Dunkl I., Antolín B., Wemmer K., Rantitsch G., Kienast M., Montomoli C., Ding L., Carosi R., Appel E., El Bay R., Xu Q., Von Eynatten H. (2011) - Metamorphic evolution of the Tethyan Himalayan flysch in SE Tibet. Geol. Soc. Spec. Publ., 353(1), 45-69, https://doi.org/10.1144/SP353.4.

Gansser A. (1964) - Geology of the Himalayas. 289 pp. Interscience Publishers, London.

Godin L., Grujic D., Law R.D., Searle M.P. (2006) - Channel flow, ductile extrusion and exhumation in continental collision zones: an introduction. Geol. Soc. Spec. Publ., 268(1), 1-23, https://doi.org/10.1144/GSL.SP.2006.268.01.01.

Goscombe B., Gray D., Hand M. (2006) - Crustal architecture of the Himalayan metamorphic front in eastern Nepal. Gondwana Res., 10(3-4), 232-255, https://doi.org/10.1016/j.gr.2006.05.003.

Grujic D., Casey M., Davidson C., Hollister L.S., Kündig R., Pavlis T., Schmid S. (1996) - Ductile extrusion of the Higher Himalayan Crystalline in Bhutan: evidence from quartz microfabrics. Tectonophysics, 260(1-3), 21-43, https://doi.org/10.1016/0040-1951(96)00074-1.

Hodges K.V. (2000) - Tectonics of the Himalaya and southern Tibet from two perspectives. Geol. Soc. Am. Bull., 112(3), 324-350, https://doi.org/10.1130/0016-7606(2000)112<324:TOTHAS>2.0.CO;2.

Hodges K.V., Parrish R.R., Housh T.B., Lux D.R., Burchfiel B.C., Royden L.H., Chen Z. (1992) - Simultaneous Miocene Extension and Shortening in the Himalayan Orogen. Science, 258(5087), 1466-1470, 10.1126/science.258.5087.1466.

Hodges K.V., Parrish R.R., Searle M.P. (1996) - Tectonic evolution of the central Annapurna Range, Nepalese Himalayas. Tectonics, 15(6), 1264-1291, https://doi.org/10.1029/96TC01791.

Johnson M.R.W., Oliver G.J.H., Parrish R.R., Johnson S.P. (2001) - Synthrusting metamorphism, cooling, and erosion of the Himalayan Kathmandu Complex, Nepal. Tectonics, 20(3), 394-415, https://doi.org/10.1029/2001TC900005.

Kohn M.J. (2008) - P-T-t data from central Nepal support critical taper and repudiate large-scale channel flow of the Greater Himalayan Sequence. Geol. Soc. Am. Bull., 120(3-4), 259-273, https://doi.org/10.1130/B26252.1.

Kohn M.J., Corrie S.L. (2011) - Preserved Zr-temperatures and U–Pb ages in high-grade metamorphic titanite: Evidence for a static hot channel in the Himalayan orogen. EPSL, 311(1-2), 136-143, 10.1016/j.epsl.2011.09.008.

Larson K.M., Bürgmann R., Bilham R., Freymueller J.T. (1999) - Kinematics of the India-Eurasia collision zone from GPS measurements. J. Geophys. Res., Solid Earth 104(B1), 1077-1093, 10.1029/1998JB900043.

Lavé J., Avouac J.P. (2000) - Active folding of fluvial terraces across the Siwaliks Hills, Himalayas of central Nepal. J. Geophys. Res., Solid Earth 105(B3), 5735-5770, https://doi.org/10.1029/1999JB900292.

Le Fort P. (1975) - Himalaya: the collided range. Am. J. Sci., 275A, 1-44.

Martin A.J., Decelles P.G., Gehrels G.E., Patchett P.J., Isachsen C. (2005) - Isotopic and structural constraints on the location of the Main Central thrust in the Annapurna Range, central Nepal Himalaya. Geol. Soc. Am. Bull., 117(7), 926, https://doi.org/10.1130/B25646.1.

Martin A.J., Ganguly J., Decelles P.G. (2010) - Metamorphism of Greater and Lesser Himalayan rocks exposed in the Modi Khola valley, central Nepal. Contrib. to Mineral. Petrol., 159(2), 203-223, 10.1007/s00410-009-0424-3.

Martin A.J., Copeland P., Benowitz J.A. (2015) - Muscovite 40Ar/39Ar ages help reveal the Neogene tectonic evolution of the southern Annapurna Range, central Nepal. Geol. Soc. Spec. Publ., 412(1), 199-220, https://doi.org/10.1144/SP412.

Molnar P., Stock J.M. (2009) - Slowing of India's convergence with Eurasia since 20 Ma and its implications for Tibetan mantle dynamics. Tectonics, 28, TC3001, https://doi.org/10.1029/2008TC002271.

Montomoli C., Iaccarino S., Carosi R., Langone A., Visonà D. (2013) - Tectonometamorphic discontinuities within the Greater Himalayan Sequence in Western Nepal (Central Himalaya): Insights on the exhumation of crystalline rocks. Tectonophysics, 608, 1349-1370, https://doi.org/10.1016/j.tecto.2013.06.006.

Montomoli C., Carosi R., Iaccarino, S. (2015) - Tectonometamorphic discontinuities in the Greater Himalayan Sequence: a local or a regional feature? Geol. Soc. Spec. Publ., 412(1), 25-41, https://doi.org/10.1144/SP412.3.

Myrow P.M., Hughes N.C., Searle M.P., Fanning C.M., Peng S.-C. Parcha S.K. (2009) - Stratigraphic correlation of Cambrian–Ordovician deposits along the Himalaya: Implications for the age and nature of rocks in the Mount Everest region. Geol. Soc. Am. Bull., 121(3-4), 323-332, https://doi.org/10.1130/B26384.1.

Parsons A. J., Law R.D., Searle M.P., Phillips R.J., Lloyd G.E. (2016a) - Geology of the Dhaulagiri-Annapurna-Manaslu Himalaya, Western Region, Nepal. 1:200,000. J. Maps, 12(1), 100-110, https://doi.org/10.1080/17445647.2014.984784.

Parsons A. J., Ferré E.C., Law R.D., Lloyd G.E., Phillips R.J., Searle M.P. (2016b) - Orogen-parallel deformation of the Himalayan midcrust: Insights from structural and magnetic fabric analyses of the Greater Himalayan Sequence, Annapurna-Dhaulagiri Himalaya, central Nepal. Tectonics, 35(11), 2515-2537, https://doi.org/10.1002/2016TC004244.

Parsons A. J., Law R.D., Lloyd G.E., Phillips R.J., Searle M.P. (2016c) - Thermo-kinematic evolution of the Annapurna-Dhaulagiri Himalaya, central Nepal: the composite Orogenic system. Geochemistry, Geophysics, Geosystems, 17(4), 1511-1539, https://doi.org/10.1002/2015GC006184.

Passchier C.W., Trouw R.A.J. (2005) - Microtectonics. Springer-Verlag, Berlin/Heidelberg. https://doi.org/10.1007/3- 540-29359-0.

Powers P.M., Lillie R.J., Yeats R.S. (1998) - Structure and shortening of the Kangra and Dehra Dun reentrants, Sub-Himalaya, India. Geol. Soc. Am. Bull., 110(8), 1010-1027, 10.1130/0016-7606(1998)110<1010:SASOTK>2.3.CO;2.

Ramsay J.G., Huber M.I., (2002) - Folds and Fractures. 6th reprinting. 309 pp. Acad. Press, London, The techniques of modern structural geology, Vol. 2.

Searle M.P. (2010) - Low-angle normal faults in the compressional Himalayan orogen; Evidence from the Annapurna–Dhaulagiri Himalaya, Nepal. Geosphere, 6(4), 296-315, https://doi.org/10.1130/GES00549.1.

Searle M.P. (2013) - Colliding Continents: A Geological Exploration of the Himalaya, Karakoram, & Tibet. 1st ed. 438 pp. Oxford University Press, Oxford.

Searle M.P., Windley B.F., Coward M.P., Cooper D.J.W., Rex A.J., Rex D., Tingdong L., Xuchang X., Jan M.Q., Thakur V.C., Kumar S. (1987) - The closing of Tethys and tectonics of the Himalaya. Geol. Soc. Am. Bull., 98(6), 678-701, https://doi.org/10.1130/0016-7606(1987)98<678:TCOTAT>2.0.CO;2.

Shrestha S., Larson K.P., Martin A.J., Guilmette C., Smit M.A., Cottle J.M. (2020) - The Greater Himalayan Thrust Belt: Insight into the assembly of the exhumed Himalayan Metamorphic Core, Modi Khola Valley, Central Nepal. Tectons, 39(9), https://doi.org/10.1029/2020TC006252.

Tapponnier P., Peltzer G., Le Dain A.Y., Armijo R., Cobbold P. (1982) - Propagating extrusion tectonics in Asia: New insights from simple experiments with plasticine. Geology, 10(12), 611-616, https://doi.org/10.1130/0091-7613(1982)10<611:PETIAN>2.0.CO;2.

Upreti B.N. (1999) - An overview of the stratigraphy and tectonics of the Nepal Himalaya. J. Asian Earth Sci., 17(5-6), 577-606, https://doi.org/10.1016/S1367-9120(99)00047-4.

Upreti B.N., Le Fort P. (1999) - Lesser Himalayan crystalline nappes of Nepal: Problems of their origin. In: Himalaya and Tibet: Mountain Roots to Mountain Tops. Geol. Soc. Am., Spec. Pap., 328, 225-238, https://doi.org/10.1130/0-8137-2328-0.225.

Upreti B.N., Yoshida M., Tribhuvana Viśvavidyālaya (EDS) (2005) - Geology and natural hazards along the Kaligandaki Valley, Nepal. 165 pp. Dept. Of Geology, Tribhuvan University, Kathmandu, Guidebook for Himalayan trekkers.

Vannay J.-C., Grasemann B. (2001) - Himalayan inverted metamorphism and syn-convergence extension as a consequence of a general shear extrusion. Geol. Mag., 138(3), 253-276, https://doi.org/10.1017/S0016756801005313.

Webb A.A.G., Yin A., Harrison T.M., Célérier J., Burgess W.P. (2007) - The leading edge of the Greater Himalayan Crystalline complex revealed in the NW Indian Himalaya: Implications for the evolution of the Himalayan orogen. Geology, 35(10), 955, https://doi.org/10.1130/G23931A.1.

Whitney D.L., Evans B.W. (2010) - Abbreviations for names of rock-forming minerals. Am. Min., 95(1), 185-187, https://doi.org/10.2138/am.2010.3371.

Yin A., Harrison T.M. (2000) - Geologic evolution of the Himalayan-Tibetan Orogen. Annu. Rev. Earth Planet. Sci., 28(1), 211-280, https://doi.org/10.1146/annurev.earth.28.1.211.

Manuscript received 08 April 2025; accepted 14 June 2025; published online XX June 2025;
editorial responsibility and handling by P. Haproff.